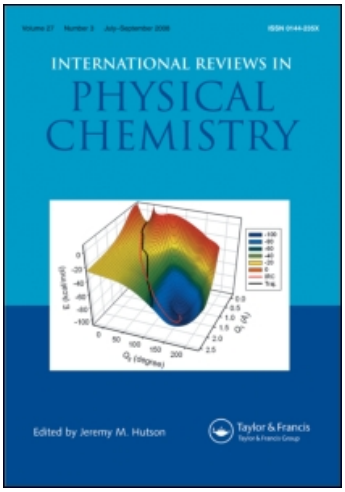

International Reviews in Physical Chemistry
Publication details, including instructions for authors and subscription information:
http://www.informaworld.com/smpp/title~content=t713724383

Spectroscopic determination of ground and excited state vibrational potential energy surfaces

Jaan Laane

Online publication date: 26 November 2010

To cite this Article Laane, Jaan(1999) 'Spectroscopic determination of ground and excited state vibrational potential energy surfaces', International Reviews in Physical Chemistry, 18: 2, 301 — 341
To link to this Article: DOI: 10.1080/014423599229974
URL: http://dx.doi.org/10.1080/014423599229974

INTERNATIONAL REVIEWS IN PHYSICAL CHEMISTRY, 1999, VOL. 18, NO. 2, 301–341

Spectroscopic determination of ground and excited state vibrational potential energy surfaces

JAAN LAANE
Department of Chemistry, Texas A&M University,
College Station, TX 77843, USA

Far-infrared spectra, mid-infrared combination band spectra, Raman spectra, and dispersed fluorescence spectra of non-rigid molecules can be used to determine the energies of many of the quantum states of conformationally important vibrations such as out-of-plane ring modes, internal rotations, and molecular inversions in their ground electronic states. Similarly, the fluorescence excitation spectra of jet-cooled molecules, together with electronic absorption spectra, provide the information for determining the vibronic energy levels of electronic excited states. One- or two-dimensional potential energy functions, which govern the conformational changes along the vibrational coordinates, can be determined from these types of data for selected molecules. From these functions the molecular structures, the relative energies between different conformations, the barriers to molecular interconversions, and the forces responsible for the structures can be ascertained. This review describes the experimental and theoretical methodology for carrying out the potential energy determinations and presents a summary of work that has been carried out for both electronic ground and excited states. The results for the out-of-plane ring motions of four-, five-, and six-membered rings will be presented, and results for several molecules with unusual properties will be cited. Potential energy functions for the carbonyl wagging and ring modes for several cyclic ketones in their $S_1(n,\pi^*)$ states will also be discussed. Potential energy surfaces for the three internal rotations, including the one governing the photoisomerization process, will be examined for *trans*-stilbene in both its S_0 and $S_1(\pi,\pi^*)$ states. For the bicyclic molecules in the indan family, the two-dimensional potential energy surfaces for the highly interacting ring-puckering and ring-flapping motions in both the S_0 and $S_1(\pi,\pi^*)$ states have also been determined using all of the spectroscopic methods mentioned above. Here, the effect of the electronic transition on the potential energy surface and hence the molecular structure can be ascertained.

1. Introduction

According to the Schrödinger equation, which for a one-dimensional vibrational problem with fixed reduced mass μ and vibrational coordinate x is

$$(-\hbar^2/2\mu)\,d^2\psi/dx^2 + V\psi = E\psi, \tag{1}$$

it is possible to calculate all the relevant energy levels and molecular properties for a molecule if its potential energy function V is known. Unfortunately, the Schrödinger equation is not always readily soluble, and only a few quantum mechanical systems can be analysed without computers. The harmonic oscillator problem, used to represent the vibration of a diatomic molecule and for which $V = \frac{1}{2}kx^2$, is one of the few cases that can be solved without numerical methods. This potential energy function, of course, fails to account for the anharmonicity present for real molecules. The anharmonicity correction can be achieved by using an alternative function such

0144-235X/99 $12·00

as the well-known Morse function [1]

$$V = D_e(1 - \exp(-\alpha x))^2 , \quad (2)$$

for which the energy levels can also be calculated without a computer.

The utilization of computers to help analyse data from vibrational spectra began in the 1960s with the application of the Wilson FG method [2] for normal coordinate calculations of polyatomic molecules, generally based on the quadratic force field. These types of calculations served to elucidate the complex nature of molecular vibrations and demonstrated that many vibrational motions were not as simple as previously assumed. Namely, considerable coupling was present between different types of motions. These calculations also provided a deeper understanding of the magnitudes of various types of force constants. Moreover, they led to the development of molecular mechanics calculations, such as the Allinger MM3 programs [3], which are based on optimized, transferable force constants applicable to a broad range of molecules, and which can be used to calculate structures and vibrational frequencies.

The development of meaningful *ab initio* calculations, which culminated in the 1998 Nobel Prize in chemistry, has also added another wrinkle to this picture. These calculations are now capable of predicting chemical structures quite accurately and also predicting vibrational frequencies, although not quite so accurately. The latter are typically calculated by using the Taylor's series definition of the force constants with respect to each coordinate q_i,

$$k_i = (\partial^2 V / \partial q_i^2)_0 \quad (3)$$

and then utilizing the harmonic oscillator solutions to determine the vibrational energy levels. *Ab initio* calculations can also be used to predict the energy difference between various conformations of the same molecule, and this feature is of value in comparing the theoretically and experimentally determined potential energy surfaces to be discussed below. However, since vibrational frequencies obtained from *ab initio* calculations are based on the assumption of harmonic forces, they can provide only limited insight into the types of highly anharmonic vibrations to be discussed in this review.

The complete vibrational analysis of a polyatomic molecule requires a multi-dimensional analysis. Nonetheless, selected vibrations in certain polyatomic molecules can be assumed to be separated from the other vibrations and can thus be analysed as a problem with reduced dimensionality. A classic example of this is the inversion vibration of ammonia which was considered by Dennison in 1940 [4]. This is an A_1 vibration. Although ammonia has a second A_1 vibration, the N–H symmetric stretching, the two vibrations have very different frequencies (3334 and 933 cm^{-1}) and these show almost no vibrational interaction. Hence, the ammonia inversion can be considered as an independent vibration definable by a one-dimensional vibrational potential energy function. Figure 1 shows the experimentally determined potential energy function which reproduces the observed experimental data. Several types of functions will yield a curve similar to that shown in the figure including the Manning potential [5], the mixed quartic/quadratic function [6]

$$V = ax^4 + bx^2 , \quad (4)$$

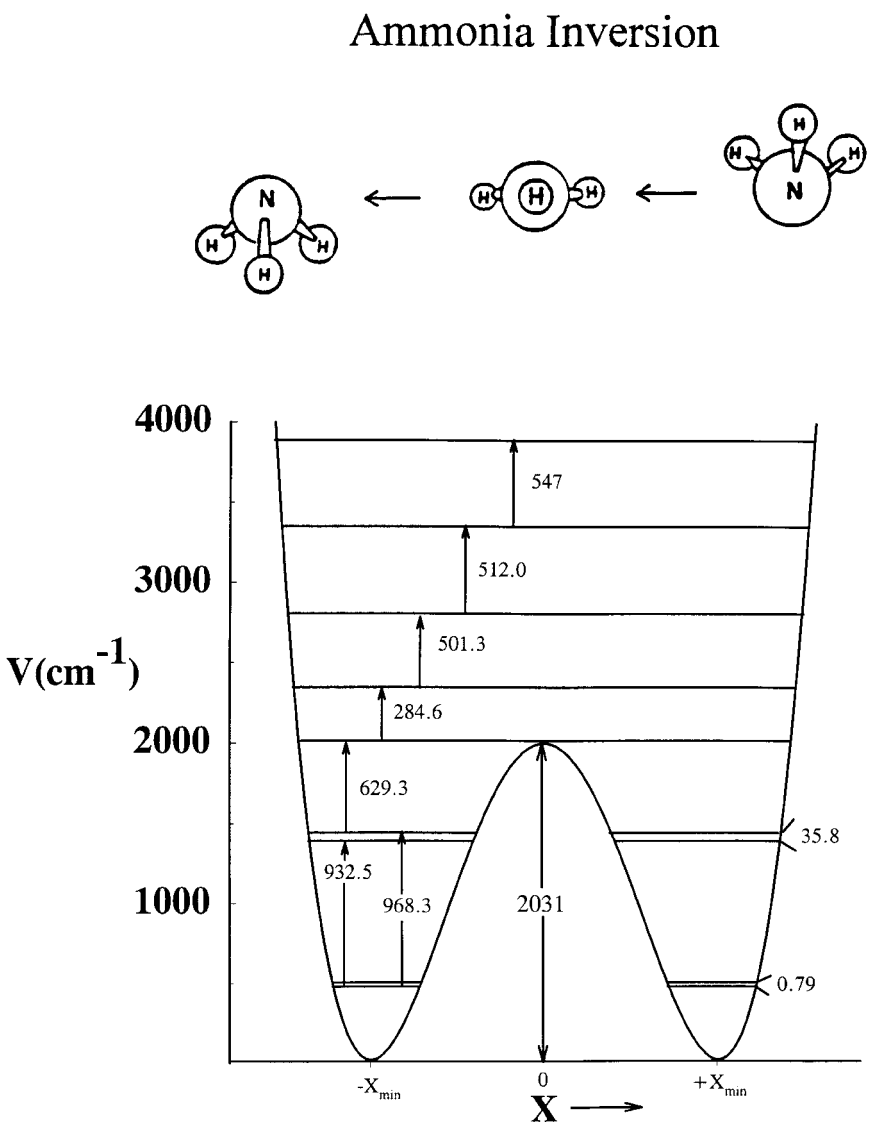

Figure 1. Potential energy function and energy levels for the ammonia inversion vibration.

which we commonly use, or the quadratic function with a Gaussian barrier [7]:

$$V = Ax^2 + B \exp(-Cx^2). \tag{5}$$

What the function in figure 1 shows is that ammonia has a pyramid structure with a barrier to inversion (a barrier to planarity) of 2031 cm^{-1} (5.80 kcal mol^{-1}). The energy minima also define the structure of the molecule based on the value of the inversion coordinate x.

For the past three decades we have been investigating the potential energy functions which govern conformational changes in non-rigid molecules [8–12]. These include the out-of-plane ring vibrations of four-, five- and six-membered rings and bicyclic ring systems, the internal rotations of molecules, and molecular inversions.

For the electronic ground state these studies have utilized far-infrared and Raman spectra of vapour-phase molecules, and more recently, the dispersed fluorescence spectra of jet-cooled molecules have also been very helpful. For electronic excited states we have recorded fluorescence excitation spectra of the jet-cooled molecules and complemented these studies with ultraviolet absorption spectra. This work has also depended on the development of computational methods for the determination of both kinetic energy and potential energy surfaces for the various types of motions.

2. Theory and computation

2.1. *Vibrational Hamiltonian*

The Hamiltonian for the vibrations of a molecule in centre-of-mass coordinates has the form

$$\mathcal{H}(q_1, q_2, \ldots) = (-\hbar^2/2) \sum_k \sum_l \partial/\partial q_k [g_{kl}(q_1, q_2, \ldots)] \partial/\partial q_l + V(q_1, q_2, \ldots) + V', \quad (6)$$

where $V(q_1, q_2, \ldots)$ is the potential energy defined in terms of the vibrational coordinates q_i. The g_{kl} are the kinetic energy (reciprocal reduced mass) expansions, and V' is the 'pseudopotential' which has been shown to be negligible [13]. The specific vibrational coordinate applicable for a particular type of molecule will be defined in the appropriate sections below. For an isolated vibrational motion like the ring-puckering, the Hamiltonian can be assumed to be one-dimensional. In other cases a two-dimensional treatment is required with q_1 and q_2 (or x_1 and x_2) representing two different vibrational coordinates. The reduction of equation (6) to a one- or two-dimensional problem is based on the approximation that all of the other vibrations in the molecule do not interact with the vibrations of interest. This has been shown to be valid in most cases, but the low-frequency modes are often not entirely uncoupled to all the other motion [8–12, 14–18].

2.2. *Calculation of kinetic energy functions*

Each vibrational coordinate of interest is represented by defining the motions of all of the atoms in the molecule in terms of that coordinate (e.g. in terms of x for the ring-puckering). We have used vector methods to define the various out-of-plane motions and developed computer calculations for the calculation of reciprocal reduced masses g_{ij} as a function of vibrational coordinates. These kinetic energy functions for one dimension have the form

$$g_{44} = g_{44}^{(0)} + g_{44}^{(2)} x^2 + g_{44}^{(4)} x^4 + g_{44}^{(6)} x^6 , \quad (7)$$

where the $g_{44}^{(k)}$ are the expansion coefficients, which are usually truncated after the 6th power term, and where $g_{44}^{(0)}$ is the reciprocal reduced mass for the $x = 0$ structure, such as the planar structure of a ring molecule. It should be noted the $i,j = 1$–3 subscripts for g_{ij} are reserved for the molecular rotations. The methodology for these calculations for various types of ring molecules has been published [19–23]. In several cases, two-dimensional kinetic energy surfaces have been computed and these will be discussed below. As an example, figure 2 shows the variation of the reciprocal reduced mass with the coordinate for the ring-puckering vibration of 1,3-disilacyclobutane [21]. The dependence of $g_{44} = 1/\mu$ on the ring-puckering coordinate x can be seen to be substantial.

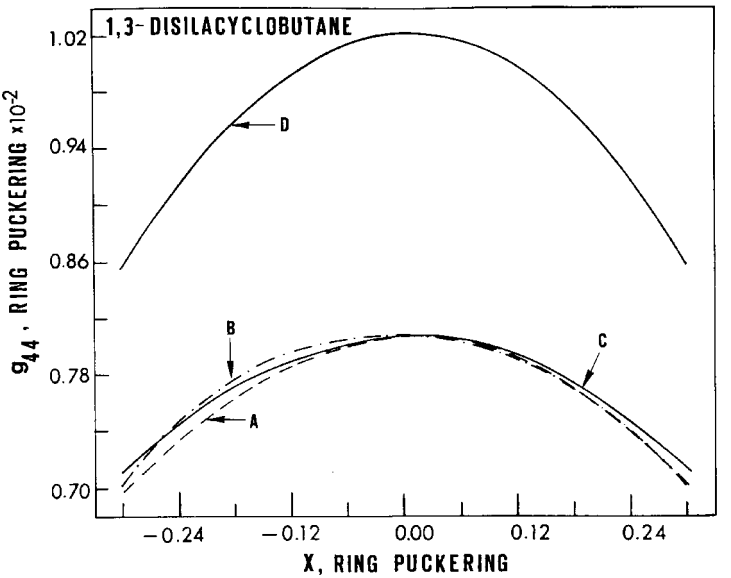

Figure 2. Dependence of the reciprocal reduced mass for the ring-puckering motion versus the puckering coordinate for several different one-dimensional (curves A, B and C) and two-dimensional (curve D) models of 1,3-disilacyclobutane [21].

2.3. *Calculation of energy levels*

Bell [24] predicted that four-membered rings should have ring-puckering vibrations which have quartic potential energy functions. Laane [25] has more recently derived the origin of this function and has shown that the angle strain in cyclobutane should give rise to a potential energy function of the form of equation (4) where the potential energy parameters are defined in terms of the ring-angle-bending force constant k_ϕ, the initial angle strain S_0, and the C–C bond distance R, by

$$a = 128k_\phi / R^4 \tag{8}$$

and

$$b = 32k_\phi S_0 / R^2 . \tag{9}$$

In addition, torsional forces will contribute to the function. For example, molecules such as cyclobutane and cyclopentene, which would have eclipsing methylene groups for their planar structures, will have substantial *negative* contributions to the quadratic term so that the constant b becomes negative.

The Schrödinger equation with a potential function of the form given in equation (4) can only be solved by numerical approximation methods. Fortunately, these matrix diagonalization techniques can give very accurate results when appropriate basis sets are used. In order to simplify the analysis of data, Laane [6] published a set of tables for determining the eigenvalues of the mixed quartic/quadratic potential function of equation (4) substituted into the Schrödinger equation (1). Utilization of these tables is simplified by use of a transformation to the reduced (undimensioned) coordinate Z:

$$Z = (2\mu / \hbar^2)^{1/6} a^{1/6} x , \tag{10}$$

where μ is the reduced mass, which here is assumed to be fixed. This results in the

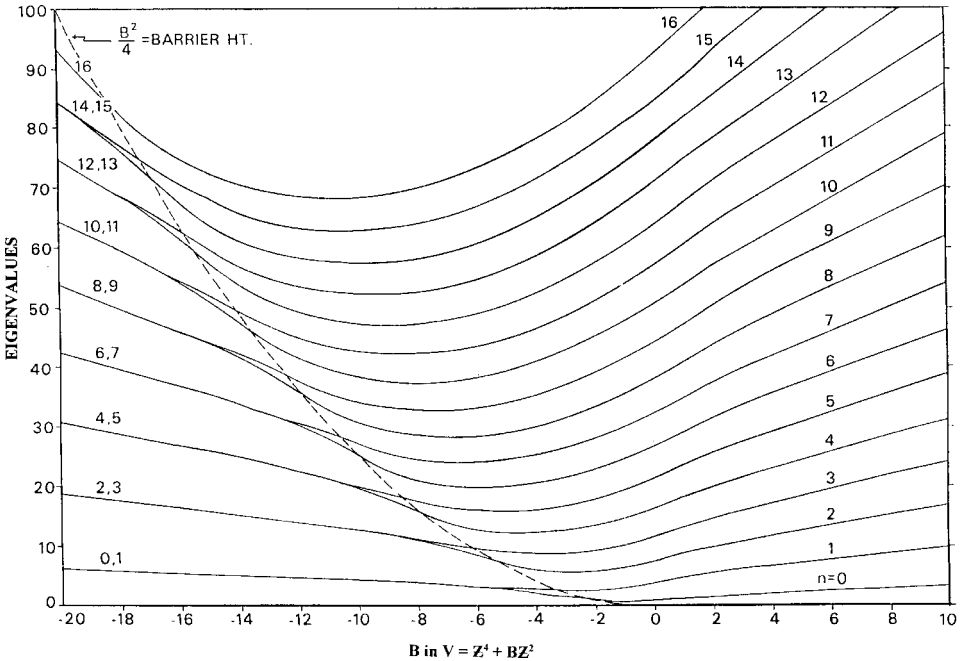

Figure 3. Variation of the eigenvalues ($\lambda = E/A$) with the reduced potential energy parameter B.

reduced Schrödinger equation

$$-\mathrm{d}^2\psi/\mathrm{d}Z^2 + (Z^4 + BZ^2)\psi = \lambda\psi, \tag{11}$$

where the energy levels E are given by

$$E = A\lambda, \tag{12}$$

where the scaling parameter is

$$A = (\hbar^2/2\mu)^{2/3}a^{1/3}, \tag{13}$$

and

$$B = (2\mu/\hbar^2)^{1/3}a^{-2/3}b. \tag{14}$$

Figure 3 shows the variation of λ versus B. When $B = 0$, pure quartic oscillator levels result. For $B > 0$ the molecule is planar with a mixed quartic/quadratic function. For negative B the potential function has a double minimum with a barrier equal to $AB^2/4 = b^2/4a$. In this region pairs of levels begin to merge and become degenerate as B becomes more negative. Thus, non-planar molecules will show irregular patterns of spectroscopic bands for the lower quantum transitions. It should be noted that use of this reduced coordinate form does not allow the incorporation of the coordinate dependence of the reduced mass as given by equation (7). Nonetheless, good approximations to the energy levels can still be attained using this procedure.

For two-dimensional problems where both vibrations are symmetric, the appropriate potential energy function is

$$V(x_1, x_2) = a_1x_1 + b_1x_1^2 + a_2x_2^4 + b_2x_2^2 + cx_1^2x_2^2, \tag{15}$$

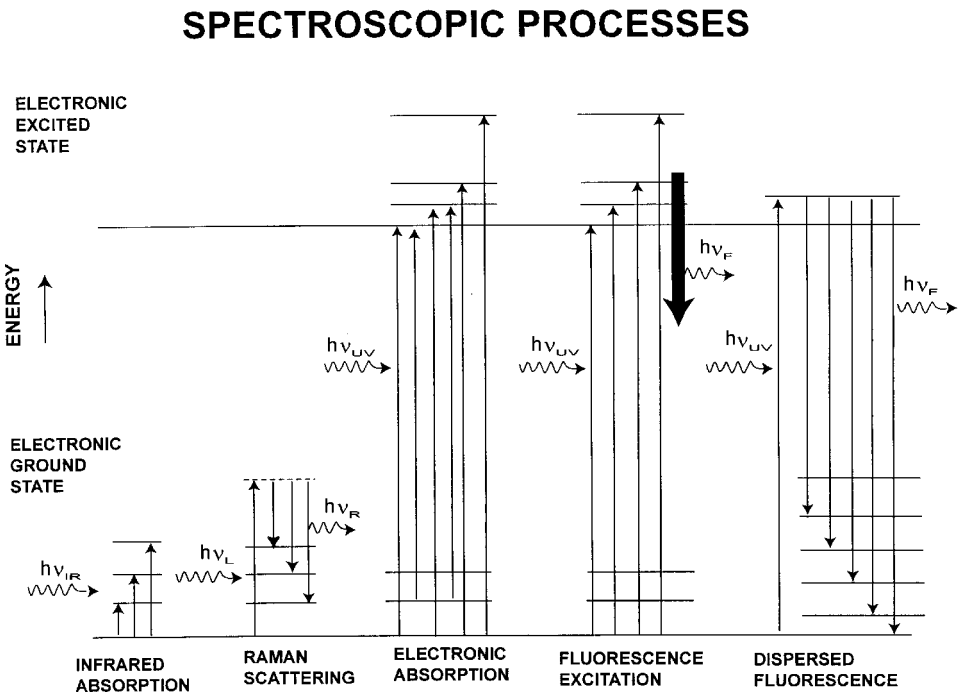

Figure 4. Spectroscopic processes used for determining vibrational quantum states in ground and excited electronic states.

where x_1 and x_2 are the two coordinates. The calculation of energy levels for this potential energy function requires the use of the product of two basis sets and the diagonalization of large matrices with typical dimensions of 500 or greater. The methods have been outlined [26] and utilized in many of our publications.

3. Experimental results

Several different spectroscopic methods have been used to determine the energies of the vibrational quantum states for the ground and excited electronic states. These are summarized in figure 4. The infrared absorption spectra, typically recorded in the far-infrared region (10 to 400 cm^{-1}), provide energy differences between electronic ground state levels, most often differing by a single quantum number ($\Delta v = 1$) although $\Delta v = 2$ and 3 transitions can also be observed. Raman spectra are recorded after laser excitation to a quasi-excited state, and the frequency shifts in the emitted Raman bands reflect energy separations between the quantum states. Quantum changes of $\Delta v = 2$ are most commonly observed since these give rise to totally symmetric transitions resulting in the more intense polarized Raman bands. The electronic absorption spectra recorded at room temperature are generally very rich and result from transitions originating from numerous ground state levels and terminating on vibronic levels in the electronic excited state. Numerous types of transitions ($\Delta v = 1$, 2, 3, 4, etc.) can be observed with symmetry and Franck–Condon factors playing important roles. We also utilize laser induced fluorescence spectroscopy of jet-cooled molecules which typically have vibrational temperatures of about 50 K so that most spectra originate from the vibrational ground state. In order to determine the vibronic energy levels in the electronic excited state

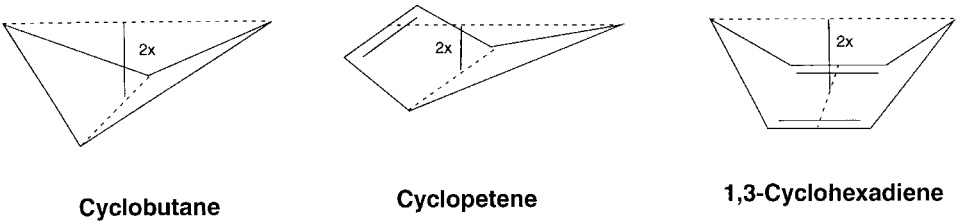

Figure 5. Definition of the ring-puckering coordinate for four- and pseudo-four-membered rings.

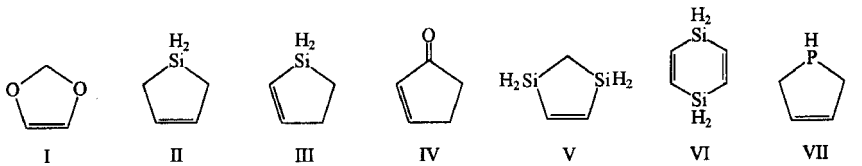

Scheme 1.

using fluorescence excitation spectroscopy, the laser is tuned through the electronic absorption region. Fluorescence occurs when the laser frequency achieves resonance with each quantum state. The dispersed, or single vibronic level fluorescence (SVLF), spectra can also be recorded to determine the energies of vibrational levels in the electronic ground state. Here, the laser is tuned into resonance with a vibronic level in the electronic excited state, and the frequencies of the emitted fluorescence bands are determined using a dispersive monochromator.

3.1. *Ring-puckering vibrations in the electronic ground state*

Following Bell's prediction [24] that a four-membered ring such as cyclobutane should have a ring-puckering vibration governed by a quartic potential energy function, the Lord group at Massachusetts Institute of Technology [27] and the Gwinn group at Berkeley [28] reported far-infrared and microwave results, respectively, for trimethylene oxide. The ring-puckering potential energy function, which is primarily quartic with a very small quadratic barrier, was reported in 1961 [29]. Shortly thereafter, the far-infrared spectra and potential functions for trimethylene sulphide and silacyclobutane were reported by Borgers and Strauss [30] and by Laane and Lord [31], respectively. Laane and Lord [32] also recognized that five-membered rings with a double bond, such as cylopentene, and six-membered rings with two double bonds, such as 1,4-cyclohexadiene [33], had ring-puckering vibrations similar to the four-membered rings. Hence, they described these rings as 'pseudo-four-membered rings'. Figure 5 shows the definition of the ring-puckering coordinate for these types of ring-systems. The distance between the ring diagonals in each case is defined as twice the coordinate x. The definition originates from the cyclobutane case where each carbon atom is assumed to be displaced either $+x$ or $-x$ from the original ring plane.

The far-infrared and/or Raman spectra of the ring-puckering of several dozen molecules have now been thoroughly analysed (scheme 1). As an example of such a study, figures 6 and 7 show the far-infrared and Raman spectra, respectively, of 1,3-dioxole (I) [34]. The far-infrared spectra primarily show $\Delta v_P = +1$ transitions

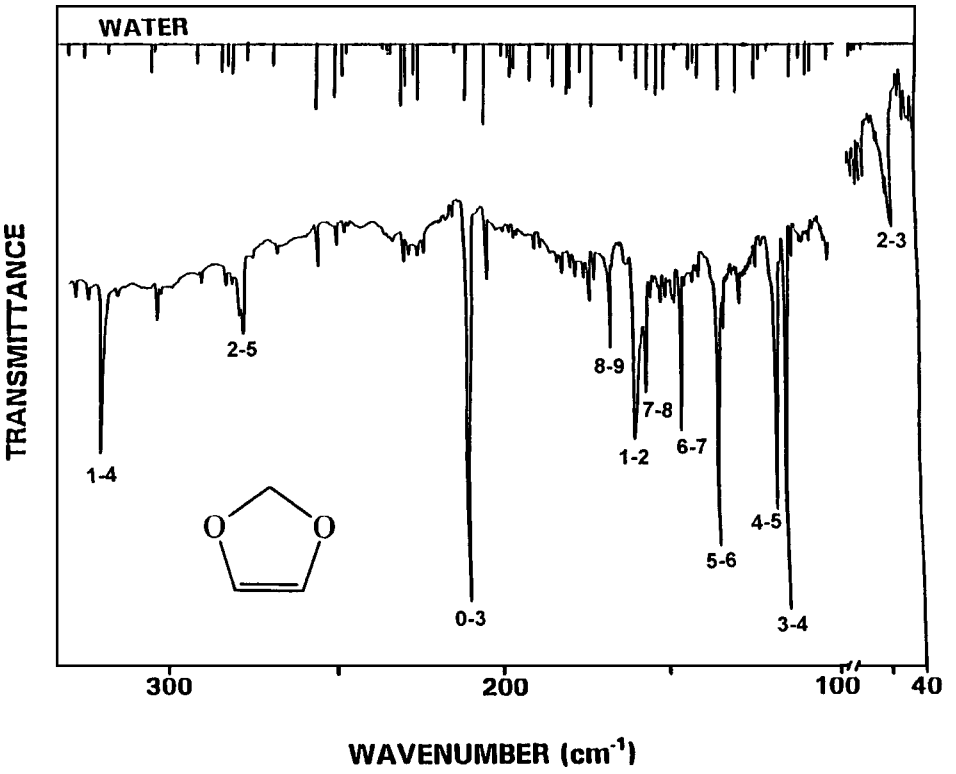

Figure 6. Far-infrared spectrum of 1,3-dioxole [34].

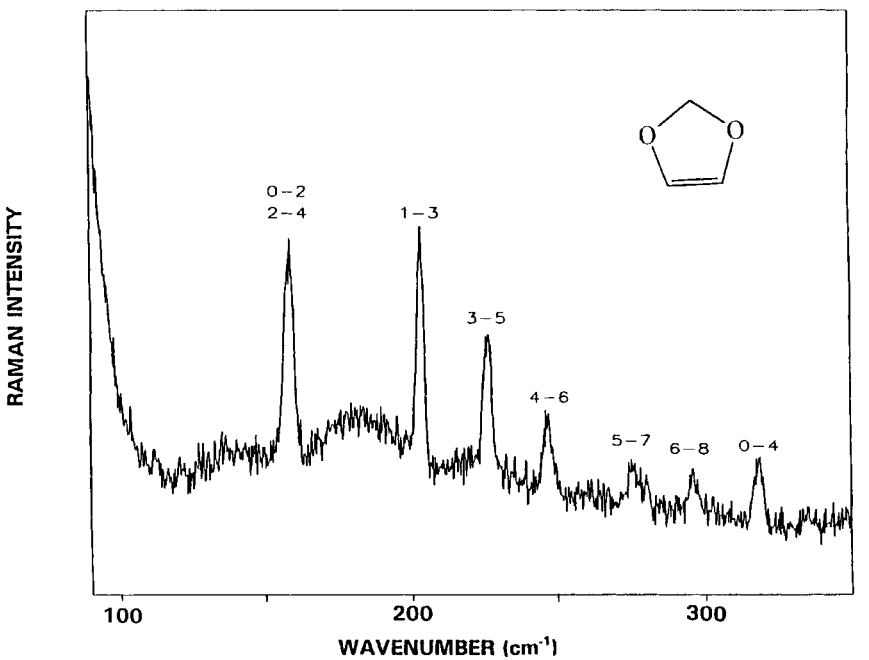

Figure 7. Raman spectrum of 1.3-dioxole [34].

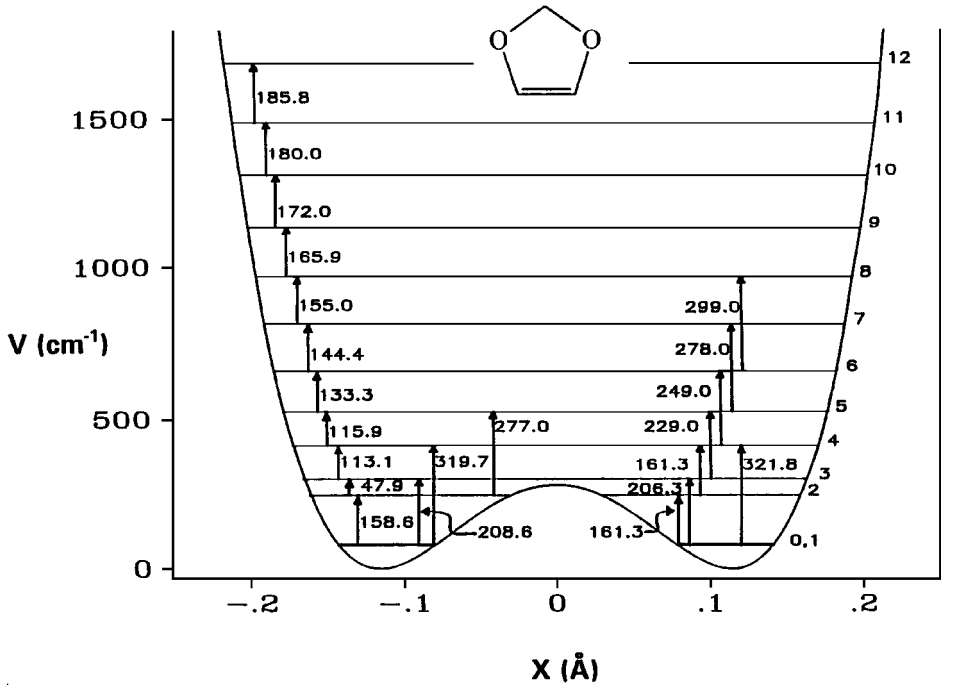

Figure 8. Ring-puckering potential energy function for 1,3-dioxole [34].

(v_P = puckering quantum number) whereas the Raman transitions are mostly $\Delta v_P = +2$. Hence, the Raman data very nicely can be used to confirm the far-infrared assignments as the Raman frequencies typically are the sums of two infrared frequencies originating from adjacent quantum states.

Figure 8 shows the ring-puckering potential energy function which has the form

$$V(\text{cm}^{-1}) = 1.59 \times 10^6 x^4 - 4.18 \times 10^4 x^2 , \quad (16)$$

where x is the puckering coordinate in Å. This potential energy corresponds to a value of $B = -5.47$ in equation (14) and figure 3. The scaling factor $A = 36.7\,\text{cm}^{-1}$. The frequencies calculated for this function have an average deviation from the observed values of only 0.7%. The barrier to planarity (or inversion) is $275\,\text{cm}^{-1}$ and the equilibrium dihedral angle is 24°. As will be shown below, this result is highly unusual since this is the only unsaturated five-membered ring molecule without any CH_2–CH_2 torsional interactions that is non-planar. In the case of 1,3-dioxole the non-planarity arises from the anomeric effect [34] present in molecules with O–C–O linkages. This effect arises from the desire of a non-bonded p orbital on an electronegative atom such as oxygen to overlap with the σ^* orbital of the C–O bond involving the other oxygen atom. Thus, the O–C–O–C= torsional angles have minimum energies at 90° and tend to twist the CH_2 group out of the plane of the rest of the molecule, forcing the ring to become puckered.

In contrast to 1,3-dioxole, silacyclopent-3-ene (II) [35, 36] is a planar molecule with a nearly purely quartic potential energy function (b is very close to zero in equation (4)). Figure 9 shows the far-infrared spectrum of this molecule [36] and figure 10 shows the ring-puckering potential energy function [35], which can

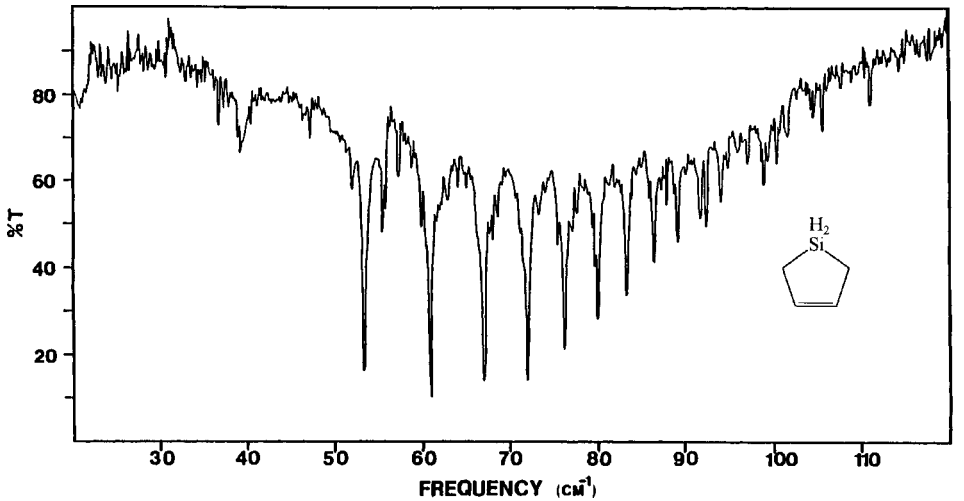

Figure 9. Far-infrared spectrum of silacyclopent-3-ene (II) [36].

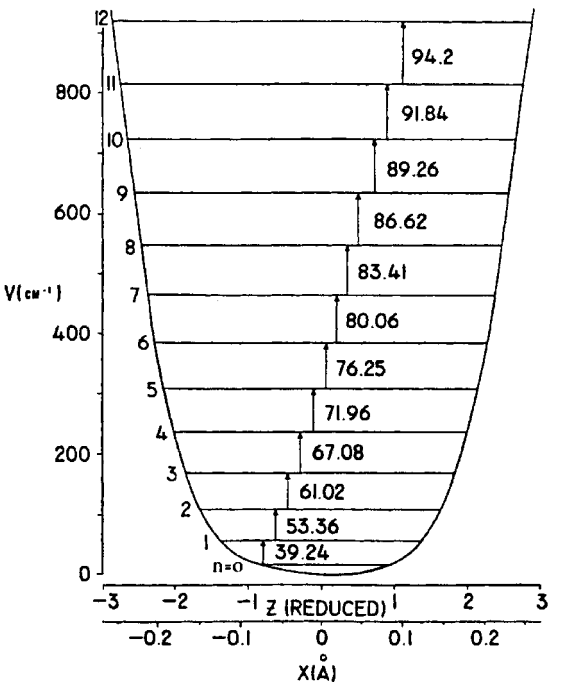

Figure 10. Ring-puckering potential energy function of silacyclopent-3-ene, a nearly perfect quartic oscillator [35].

be represented by $A = 14.34\,\mathrm{cm}^{-1}$ and $B = 0$. It should be noted that for a quartic oscillator, unlike for a harmonic oscillator, the energy levels spread apart with quantum number. As more quadratic character is added, by increasing the magnitude of coefficient b in equation (4), the energy spacings tend to approach the same value. This can be seen in figure 3 where the energy levels become harmonic

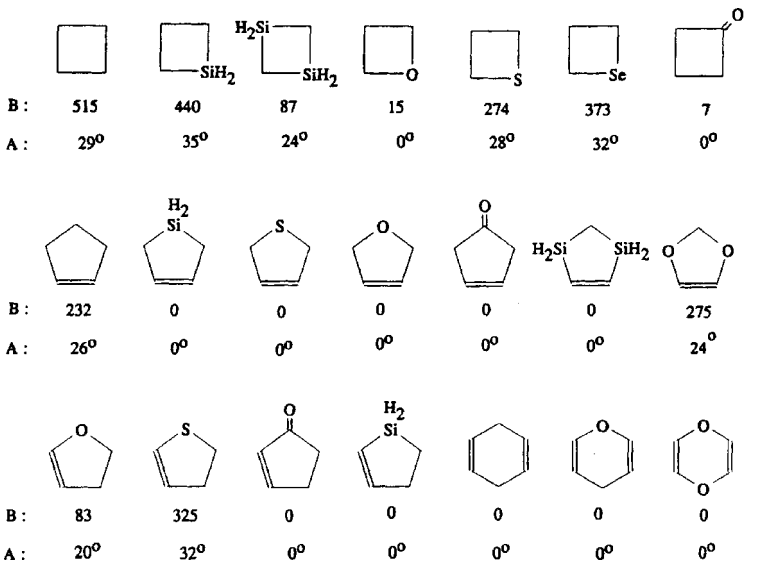

Figure 11. Barriers (B) and dihedral angles (A) for ring molecules.

as B approaches infinity. The energy minimum corresponds to the planar structure, but the puckering vibration has an amplitude of more than $\pm 20°$ for the dihedral angle so most of the time the molecule is quite puckered. The two-dimensional potential energy surface including the interaction with the ring-twisting motion has also been determined [36]. The amount of interaction is modest but accounts for the frequency shifts of about 2 cm^{-1} in the puckering bands in the ring-twisting excited state. Similar calculations have been carried out for the non-planar cyclopentene molecule [15].

Figure 11 shows inversion barriers and dihedral angles for some of the four-, five- and six-membered ring molecules for which one-dimensional potential energy functions have been determined from their low frequency vibrational data. More than half of these have been studied in our laboratory. With the exception of 1,3-dioxole (discussed above) and silacyclopent-2-ene (III), barriers and angles can be understood within the angle strain/ torsional forces context: increasing the number of CH_2–CH_2 interactions increases the barriers to planarity; decreased angle strain resulting from 'softer' atoms such as S, Se, and Si allows rings to pucker more; CH_2–SiH_2 interactions are much weaker than CH_2–CH_2 interactions, etc. Silacyclopent-2-ene [38, 39] is unusual in that it is not only planar but also very rigid despite its CH_2–CH_2 and SiH_2–CH_2 torsional interactions. The analogous oxygen and sulphur molecules have barriers of 83 and 325 cm^{-1} respectively because of the presence of single CH_2–CH_2 interactions. Silacyclopent-2-ene is more similar to 2-cyclopentenone (IV) which is planar due to the conjugation between the carbonyl and olefinic segments of the molecules. It therefore appears that a special interaction is present between the silicon atom and the carbon–carbon double bond. This may or may not be a p_π–d_π interaction. The unusual results on silacyclopent-2-ene prompted us to prepare and study 1,3-disilacyclopent-4-ene (V) [40] and 1,4-disilacyclohexa-2,5-diene (VI) [41], which we thought might also possess silicon interactions with the carbon–carbon double bonds. The far-infrared spectra of V, however, is characteristic of a planar

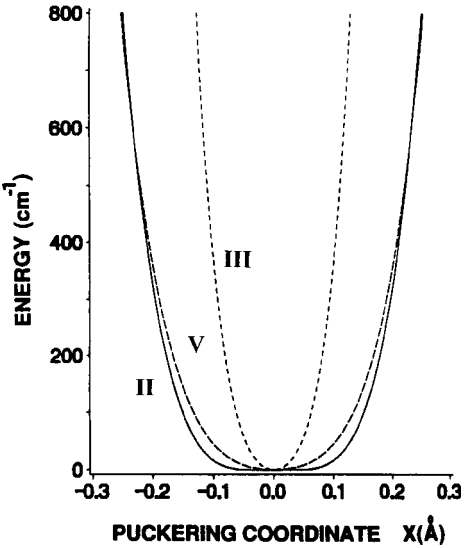

Figure 12. Ring-puckering potential energy functions for II, III and V [40].

but relatively floppy ring. A hint of some increased rigidity is present but this is much less than in the silacyclopent-2-ene. Figure 12 compares the ring-puckering potential energy functions of II, III and V. Each molecule is non-planar, but III is clearly the most rigid. For VI there is no indication at all of any special interaction as this molecule is less rigid than 1,4-cyclohexadiene [33, 40].

A number of asymmetric one-dimensional potential energy functions have also been reported for molecules such as 3-phospholene (VII) [17], for which a two-dimensional potential energy surface in terms of the ring-puckering and PH inversion has also been determined and will be shown below. Several substituted cyclobutanes and various bicyclic compounds [8–12] also possess asymmetric functions.

3.2. *Two-dimensional potential energy surfaces*

3.2.1. *Five-membered ring molecules*

As discussed above, a five-membered ring molecule with a double bond (e.g. cyclopentene) is a pseudo-four-membered ring molecule with a ring-puckering vibration that may be assumed to be independent from all the other vibrational modes, including the ring twisting, which involves twisting of the double bond. For saturated five-membered rings, however, both the twisting and bending (puckering) motions must be considered. Pitzer and co-workers [42] showed that the vibrations of cyclopentane are better represented by a radial motion q (sometimes labelled r) and a pseudorotation angle ϕ rather than by the bending and twisting coordinates. Figure 13 shows the various twisted and bent conformations of cyclopentane that arise as the pseudorotational phase angle ϕ changes. For unhindered pseudorotation the levels are given by

$$E = n^2 B \text{ for } B = \hbar^2 / 2mq_0^2 \text{ and } n = 0, 1, 2, \ldots , \tag{17}$$

where m is the effective mass of a methylene group in cyclopentane and q is the equilibrium value of the radial coordinate which measures motion out of the ring plane. Durig and Wertz [43] originally observed pseudorotational combination bands

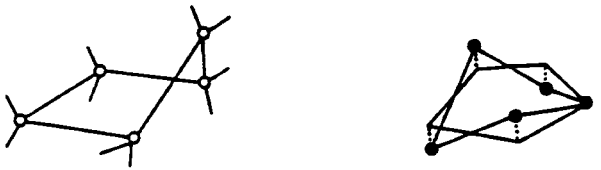

C_s, Envelope

BENT(B)

C_2, Half-chair

TWISTED(T)

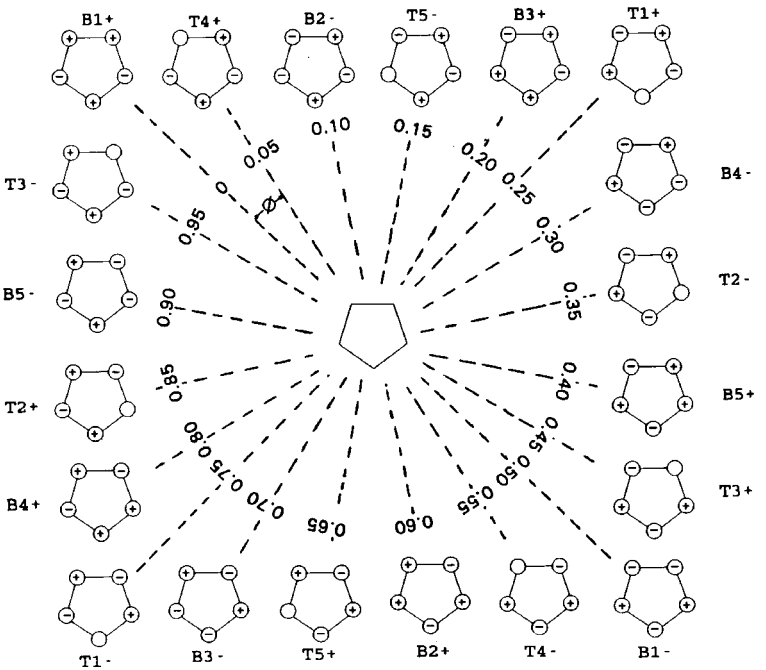

Figure 13. Conformations of cyclopentane shown at $\pi/10$ intervals for different pseudorotational phase angles ϕ.

arising from a CH_2 deformation mode. The same bands recorded in our laboratory under higher resolution [44] are shown in figure 14. Based on the model given by equation (17), the pseudorotational constant B was determined to be 2.60 cm^{-1}. A more comprehensive two-dimensional analysis in terms of the bending and twisting coordinates resulted in the potential energy surface shown in figure 15 [44]. The phase angle given in figure 13 can be correlated with the various cyclopentane structures along the energy minimum, which is the pseudorotational pathway. There is essentially free pseudorotation and the barrier to planarity is 5.2 kcal mol^{-1}.

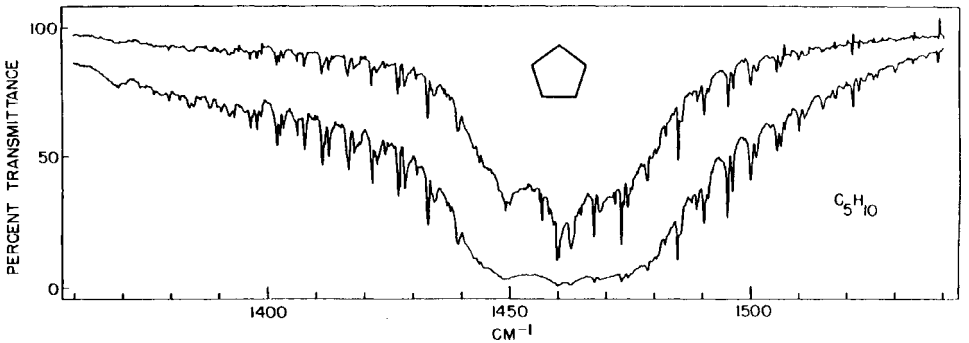

Figure 14. Pseudorotational combination bands of cyclopentane [44].

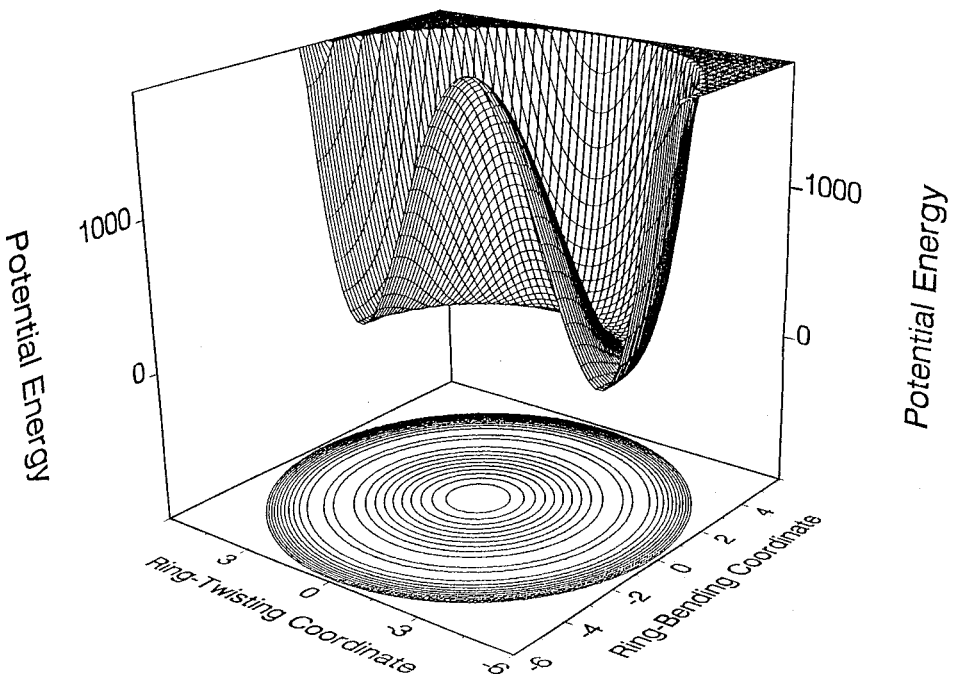

Figure 15. Potential energy surface for the ring-bending and twisting motions of cyclopentane.

When a hetero atom is introduced into the cyclopentane ring, as in silacyclopentane, a barrier to pseudorotation results since the bent and twisted forms have considerably different energies. The two-dimensional potential energy surface is then best examined in terms of ring-bending and twisting coordinates. Figure 16 shows the ring-bending spectrum of silacyclopentane and figure 17 shows the energy map determined from the bending, twisting, overtone, and combination band spectra [45]. Figure 18 presents the two-dimensional potential energy surface defined by a function of the form given in equation (15). The surface shows that silacyclopentane has a twisted structure 2050 cm^{-1} lower in energy than the planar form. The bent conformation corresponds to a saddle point on the surface. It is 1400 cm^{-1} higher

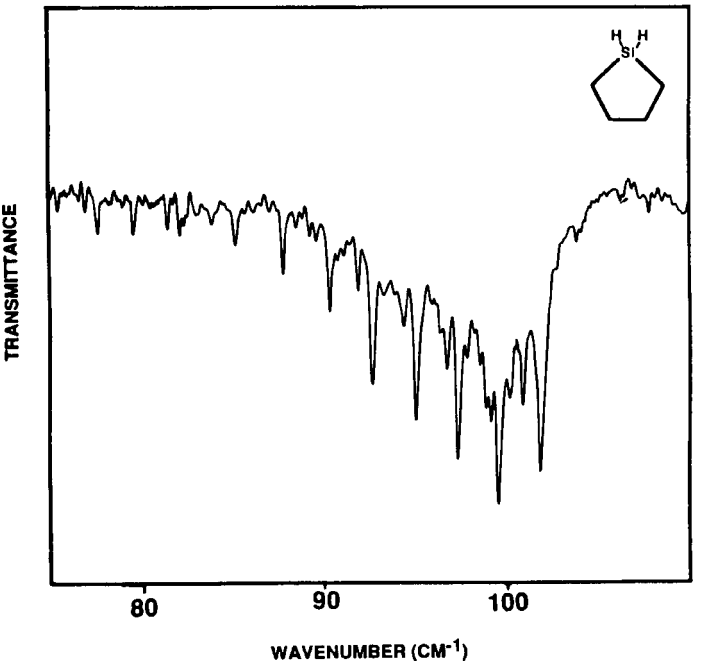

Figure 16. Far-infrared spectrum of silacyclopentane in the ring-bending region [45].

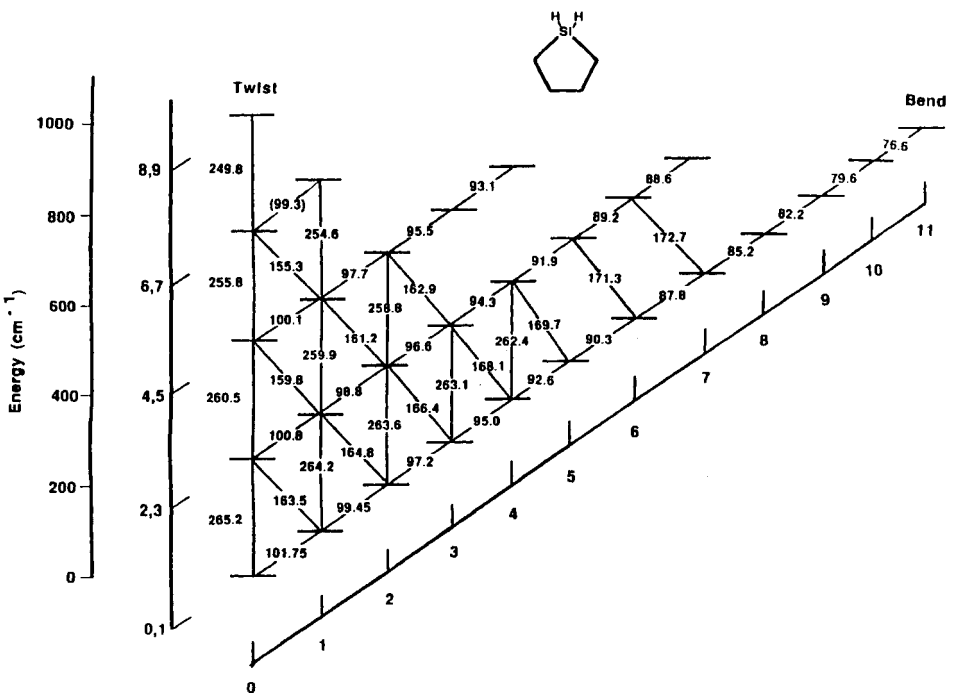

Figure 17. Energy levels and transitions for the ring-bending and twisting vibrations of silacyclopentane [45].

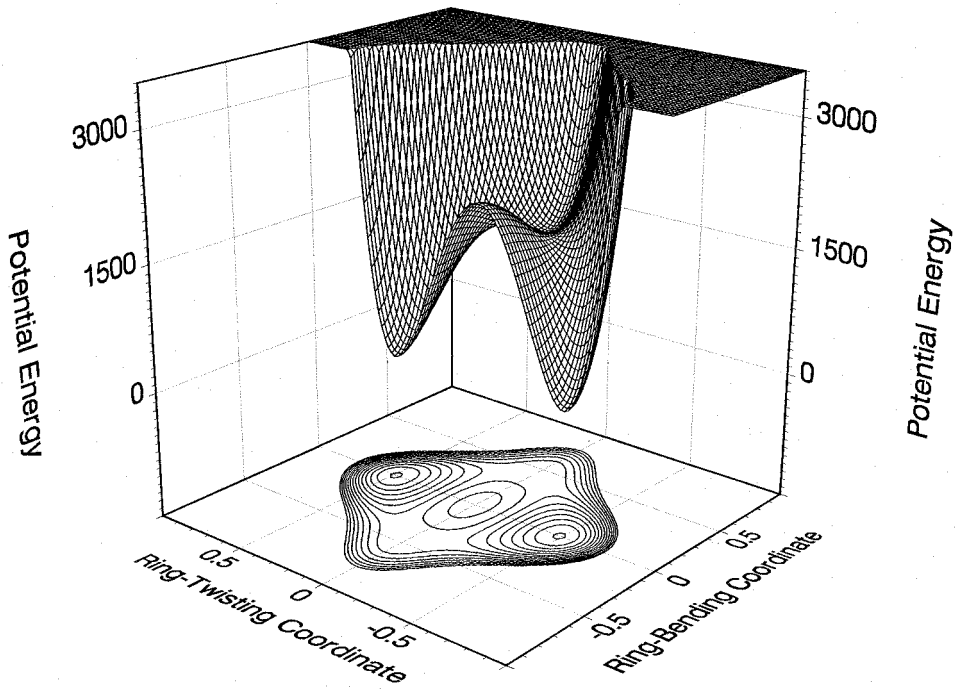

Figure 18. Two-dimensional potential energy surface for the out-of-plane ring-bending and twisting of silacyclopentane [45].

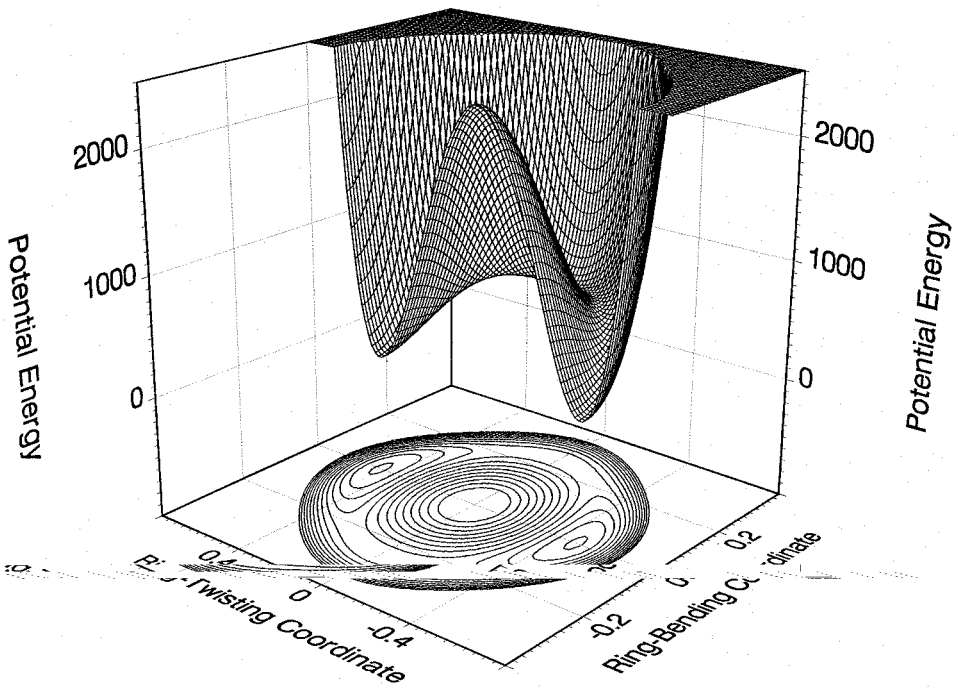

Figure 19. Two-dimensional potential energy surface for the bending and twisting of 1,3-oxathiolane [48].

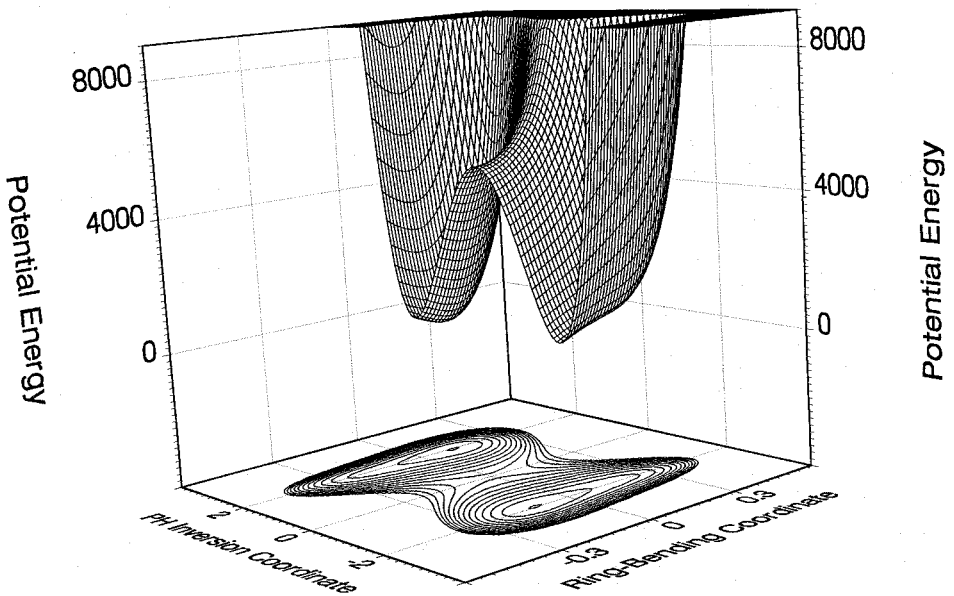

Figure 20. Two-dimensional potential energy surface for the ring-bending and PH inversion of 3-phospholene (VII) [18].

in energy than the twisted conformation, and this value represents the barrier to pseudorotation. As can be seen in figure 17, each of the energy levels below the barrier is two-fold degenerate due to the two equivalent twisting minima in the potential energy surface.

Another interesting molecule with hindered pseudorotation is 1,3-oxathiolane [46–48]. Figure 19 shows the two-dimensional potential energy surface determined from the far-infrared spectrum of this molecule. The anomeric effect is also operational here and serves to decrease the energy of the bent conformation. The barrier to planarity is 2289 cm^{-1}, but the barrier to pseudorotation is only 570 cm^{-1}. The low barrier to pseudorotation allows the ring-bending energy levels to be calculated quite well using a one-dimensional pseudorotational potential energy function in terms of the pseudorotational phase angle ϕ shown in figure 13 [46].

The potential energy surface for 3-phospholene [18] is quite different in that it is defined in terms of the bending and PH inversion coordinates. Because the phosphorus hydrogen lies above the ring plane and because the ring is puckered, this surface is less symmetrical than that for silacyclopentane. The surface determined from the far-infrared and combination band spectra is shown in figure 20. There are two equivalent puckering minima each with the same amount of PH inversion. Inversion or puckering from the minimum energy conformation does not produce another minimum. The barrier to total planarity of both the ring and PH group is about 6000 cm^{-1}.

3.2.2. *Cyclohexene and related molecules*

We have also analysed the far-infrared spectra of cyclohexene and several of its deuterated isotopomers [49]. In addition, the spectra of several analogues containing oxygen [50] or sulphur [51] atoms in the rings were also studied in order to

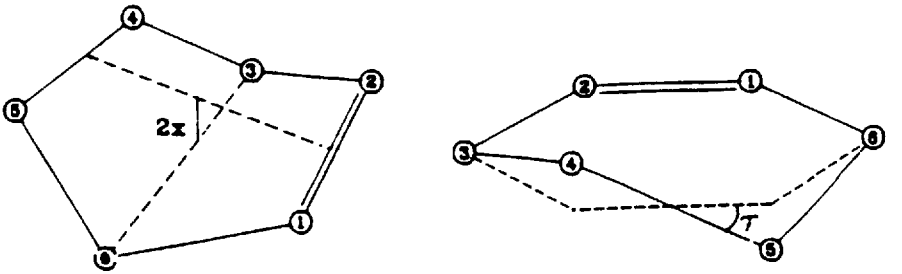

Figure 21. Ring-bending (x) and ring-twisting (τ) coordinates for cyclohexene [52].

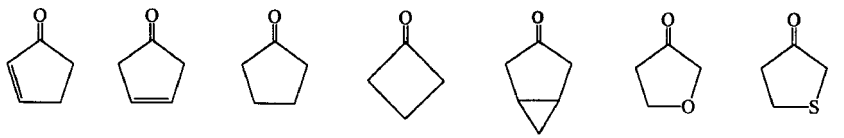

2CP 3CP CP CB BCH THFO THTP

Scheme 2.

determine their potential energy surfaces. Figure 21 defines the bending and twisting coordinates used for each potential energy surface. The two-dimensional surface determined for cyclohexene from the vibrational data for five different isotopic species is qualitatively very similar in appearance to that of silacyclopentane in figure 18 where the minima correspond to twisted structures and the saddle points correspond to the bent conformations. Quantitatively the barriers to planarity and interconvsersion are much higher for cyclohexene. Table 1 summarizes the data for the six molecules of this type which we have investigated. The energy differences determined are consistent with expectations based on angle strain, torsional effects and anomeric effects [49–51]. In each case the molecule is twisted with a barrier to planarity of 3500 cm^{-1} to 4700 cm^{-1}. The pathway to interconversion from one twist form to another crosses the saddle point and involves a substantial barrier. Hence, the interconversion process, which can be viewed as a hindered pseudorotation, does not occur readily.

3.3. *Fluorescence spectra of cyclic ketones*

In recent years, the combination of tunable high power lasers and pulsed supersonic jet techniques have provided the means of obtaining high resolution electronic spectra that are greatly simplified due to the sample cooling provided by the supersonic jet. The cooling results in the removal of hot bands and the narrowing of the bandwidths for the remaining bands. The lack of spectral congestion allows a much more accurate and thorough analysis of the low-frequency vibrations in electronic excited states than previously possible using fluorescence or absorption techniques. The experimental procedures utilized by us have been previously described [52–54].

A number of carbonyl compounds (scheme 2) have been analysed by electronic absorption spectroscopy over the years, but in many cases the complexity of the spectra made it nearly impossible to attain the correct interpretation of the spectra. We have recently investigated a number of cyclic ketones in their $S_1(n,\pi^*)$ states. In this electronic state, a carbonyl compound typically distorts from a planar to a

Table 1. Two-dimensional potential energy functions[a] for the ring-bending and ring-twisting of cyclohexene and analogues.

	a_1(cm^{-1}Å^{-4})	b_1(cm^{-1}Å^{-2})	a_2(cm^{-1}rad^{-4})	b_2(cm^{-1}rad^{-2})	c(cm^{-1}(Å^{2}rad^{-2})$^{-1}$)	B_{pt}(IR)[b]	B_{int}(IR)[c]
$CH_2CH_2CH{=}CH\,CH_2CH_2$	3.25×10^4	-1.19×10^4	2.18×10^4	-2.02×10^4	1.53×10^5	4700	3600
$CH_2CH_2CH{=}CHOCH_2$	4.24×10^4	-1.01×10^4	2.46×10^4	-2.00×10^4	1.70×10^5	4080	3480
$CH_2OCH{=}CHOCH_2$	15.9×10^4	-1.39×10^4	2.92×10^4	-2.20×10^4	1.96×10^5	4130	3830
$CH_2CH_2CH{=}CHCH_2O$	5.99×10^4	-1.19×10^4	2.29×10^4	-2.04×10^4	1.91×10^5	4130	3540
$CH_2OCH{=}CHCH_2O$	7.08×10^4	-1.04×10^4	3.31×10^4	-2.23×10^4	2.44×10^5	3500	3120
$CH_2CH_2CH{=}CHCH_2S$	2.43×10^4	-0.38×10^4	2.26×10^4	-1.97×10^4	1.03×10^5	4280	4130

[a] $V(x, \tau) = a_1x^4 + b_1x^2 + a_2\tau^4 + b_2\tau^2 + cx^2\tau^2$, where x and τ are the ring-bending and ring twisting coordinates, respectively.
[b] B_{pt} = barrier to planarity = $E_{plane} - E_{twist}$.
[c] B_{int} = barrier to interconversion = $E_{bent} - E_{twist}$.

pyramidal configuration about the carbonyl carbon atom. This was predicted for formaldehyde in 1953 by Walsh [55] and verified spectroscopically by Brand in 1956 [56]. In our investigations we have determined the carbonyl wagging potential energy functions for the cyclic ketones shown in scheme 2, and also examined their conformationally important out-of-plane ring motions wherever possible.

Cheatham and Laane [57] have carried out a reanalysis of the ring-puckering and ring-twisting far-infrared spectra of 2-cyclopenten-1-one (2CP) and two of its isotopomers. The puckering and twisting states, along with many combination states, were well defined, and a two-dimensional vibrational potential energy surface was determined in terms of these two large-amplitude motions. This detailed knowledge of the ground state energy levels was essential for the analysis of the electronic excited state. Cheatham and Laane [58] also recorded the $S_1(n,\pi^*)$ laser-induced fluorescence excitation spectra of two isotopic forms of jet-cooled 2CP and reassigned many of the low-frequency vibrational bands in the excited state. The determination of the ring-puckering levels made it possible to establish the vibrational potential energy function for this motion, and thus the molecular conformation, in the electronic excited state. The ring-twisting and carbonyl-bending motions were also identified. In both the ground and excited electronic states 2CP is planar and hence has a single minimum ring-puckering potential energy function in each case. However, the puckering frequency drops from 94 cm^{-1} in the ground state to 67 cm^{-1} in the $S_1(n,\pi^*)$ state, reflecting a floppier ring system in the excited state resulting from the decreased conjugation following the n to π^* transition. The decreased conjugation also results in the C=O and C=C stretching frequencies decreasing from 1784 to 1357 cm^{-1} and 1599 to 1418 cm^{-1}, respectively. Table 2 lists some of the frequency data for 2CP as well as for the other molecules to be discussed below.

For the three ketones, 3-cyclopenten-1-one (3CP), cyclopentanone (CP) and cyclobutanone (CB), each molecule has C_{2v} symmetry for a planar structure for which the purely electronic transition is symmetry forbidden ($^1A_2 \leftarrow {}^1A_1$). There is no conjugation in these molecules, and thus the carbonyl group is not expected to remain co-planar with the ring system in any of these molecules as it does for 2CP. Sufficient data for the out-of-plane C=O wagging motion for each molecule was obtained so that we could determine the double-minimum potential energy functions which govern these vibrations.

Figure 22 shows the jet-cooled fluorescence excitation spectrum [59] of 3-cyclopenten-1-one (3CP). The band origin is observed at 30 238 cm^{-1}. Each $v = 0$ (in the electronic ground state) to $v = n$ (in the A_2 electronic excited state) transition of the C=O wag has B_2 vibrational symmetry (assuming the molecule to lie in the *xz* plane) for $n =$ odd, but has A_1 vibrational symmetry for $n =$ even. Only transitions to the $n =$ odd states can be observed. These show up as intense Type B bands arising from $A_2 \times B_2 = B_1$ symmetry. The first five of these transitions are labelled in figure 22. It should be noted that since the $v = 0$ and $v = 1$ levels in the $S_1(n,\pi^*)$ state are near-degenerate, the band origin lies very close to the $0 \rightarrow 1$ frequency. The other bands in the spectrum include many combinations of the C=O wag with the ring-puckering vibration and combinations of these with other fundamentals including the C=O stretch. Of particular note is the $3_0^1 29_0^4 30_0^1$ band at 32 211 cm^{-1}, shifted 1973 cm^{-1} from the band origin and 746 cm^{-1} from the C=O stretching (ν_3) value at 1227 cm^{-1}. The 1973 cm^{-1} value corresponds to the sum of ν_3, of the $0 \rightarrow 4$ wagging transition (ν_{29}), and of the ring-puckering (ν_{30}) frequency of 127 cm^{-1}. This shows the $0 \rightarrow 4$ spacing to be 619 cm^{-1}, which is 21 cm^{-1} less than the $0 \rightarrow 5$ spacing.

Table 2. Comparison of frequencies of several vibrations of cyclic ketones in the ground and $S_1(n,\pi^*)$ electronic excited states.

	2CP		THTP		CP		BHO		3CP		THFO		CB	
Vibration	S_0	S_1	S_0	S_1	S_0	S_1	S_0	S_1	S_0	S_1	S_0	S_1	S_0	S_1
Ring puckering	94	67	67	58	95	91	86	134	83	127	59	82	36	106
Ring twisting	287	274	170	–	38	238	–	–	378	377	228	224	–	–
C=O wag (o.p.)	537	422	427	326	446	309	–	315	450	336	463	344	395	355
C=O wag (i.p.)	464	348	483	329	467	342	–	–	458	339	463	365	454	392
C=O stretch	1748	1357	1760	1240	1770	123	–	–	1773	122	1755	1232	1816	125

i.p., in plane. o.p., out of plane.

Table 3. Potential energy parameters and reduced masses C=O wagging vibrations in the $S_1(n,\pi^*)$ electronic state.

		$V = ax^4 + bx^2$		$V = A(z^4 + Bz^2)$				
Molecule	v(au)	a(cm^{-1}Å^{-4})	b(cm^{-1}Å^{-2})	A(cm^{-1})	B	Barrier (cm^{-1})	ϕ_{min}	Reference
CP	5.569	10.49×10^3	-5.34×10^3	45.8	−7.70	672	22°	[60]
3CP	5.157	8.82×10^3	-5.75×10^3	45.5	−9.08	939	24°	[59]
CB	4.245	2.12×10^3	-4.72×10^3	31.7	−18.20	2149	39°	[62]
THFO	5.208	8.51×10^3	-6.26×10^3	44.7	−10.15	1151	26°	[63]
THTP	3.572	13.4×10^3	-5.94×10^3	66.8	−5.47	659	20°	[63]
BCH[a]	6.49	7.84×10^3	-5.18×10^3	37.5	−9.55	873	23°	[54]

[a] The asymmetric term $0.097 \times 10^3 x^3$ is also included.

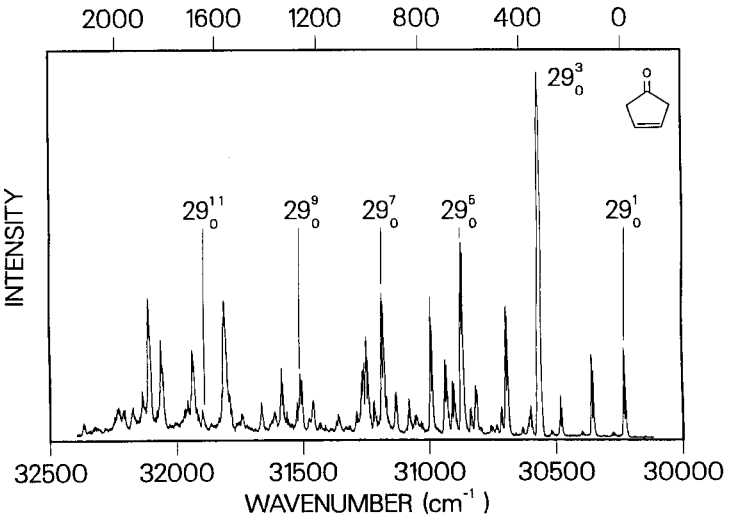

Figure 22. FES of 3-cyclopenten-1-one [59].

In order to analyse the C=O wagging vibration in the electronic excited state, we have utilized our computer programs, described previously, for calculating the reduced masses [21, 59] and energy levels [6, 26] for the Schrödinger equation (1) and the potential energy function given by equation (4). Here x is used for the C=O wagging coordinate given in terms of the wagging angle ϕ and the C=O bond distance R by [20]

$$x = R\phi\,. \tag{18}$$

The reciprocal reduced mass expansion g_{44} for this coordinate has the form given in equation (7) and is given elsewhere [59].

For 3CP the reduced mass and the carbonyl wagging potential energy parameters which best fit the observed frequency separations are given in table 3 along with similar data for the other cyclic ketones discussed below. The experimentally determined potential energy function in the form of both equations (4) and (5) is shown in figure 23 along with the observed frequency separations. The minimum energy corresponds to a wagging angle of $\pm 24°$ and the barrier to inversion is 939 cm^{-1} (2.65 kcal mol^{-1}). Although equations (4) and (5) represent potential energy functions which are primarily quartic or quadratic, respectively, above the barrier, the calculated potential energy levels below the barrier are very similar as long as the potential energy parameters result in the same barrier height and energy minima. For 3CP the ring-puckering frequency of 127 cm^{-1} in the S_1 state is considerably higher than the value of 83 cm^{-1} in the ground state. This is due in part to the asymmetry that is associated with this motion in the excited state.

The survey spectrum of cyclopentanone (CP) [60] is shown in figure 24. The band origin is at 30 276 cm^{-1}. In the ground state this molecule is twisted [61] and, in the C_{2v} approximation, the vibrational ground state is nearly doubly degenerate with symmetry species A_1 and A_2. The twisting conformation (and degeneracy) carries through to the electronic excited state as demonstrated by the similarity in the ring-bending and twisting frequencies in the S_1 state. The purely electronic transition is again $^1A_2 \leftarrow {}^1A_1$ which is forbidden in the C_{2v} approximation. However,

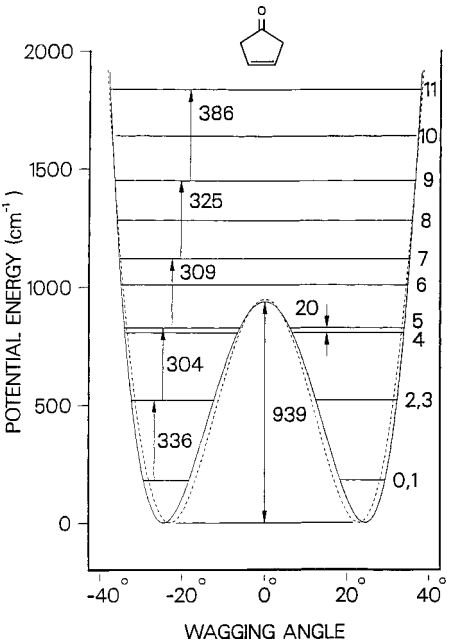

Figure 23. Vibrational potential energy function for the C=O wagging vibration of 3CP [59]. The solid curve has the form of equation (4); dashed line: equation (5).

combination with odd quantum transitions of the $\nu_{25}(B_2)$ C=O wagging results in Type B bands from B_1 symmetry. If either the ground or excited electronic state also is in combination with the near-degenerate $\nu_{18}(A_2)$ twisting state, the even quanta C=O wagging transitions can also be observed as Type A (A_1) bands ($A_2 \times A_2 \times (B_2)^n = A_1$ for n = even). Figure 24 shows that transitions for both even and odd quantum states of the C=O wag in the S_1 state are readily observed.

Figure 25 shows the C=O wagging potential energy function for CP with a barrier of 680 cm^{-1} and the energy minima at $\pm 22°$. The kinetic and potential energy terms are given in table 3. The comparison between the S_0 and S_1 states for the fundamental vibrational frequencies of several other modes is given in table 2.

The fluorescence excitation spectrum (FES) of CP has sufficient detail that it was possible to assign many of the excited states of the out-of-plane ring vibrations in addition to the carbonyl wagging modes. Figure 26 shows the energy level diagram for the ring-twisting, carbonyl wagging, and ring-bending modes for both the ground state [61] and the S_1 excited state. This data made it possible to determine the two-dimensional potential energy surfaces for the ring-bending and twisting modes for both electronic states and these are both shown in figure 27. In both states the molecule has a twisted conformation, but in the S_1 excited state the bent conformations are greatly reduced in energy due to the decreased angle strain at the carbonyl carbon atom. Nevertheless, these conformations are only saddle points on the surface and do not represent stable conformations. For both electronic states the barrier to planarity is approximately 1400 cm^{-1}.

The fluorescence excitation spectrum of cyclobutanone (CB) [62] is shown in figure 28 with the band origin at 30 292 cm^{-1}. Only transitions involving the odd quantum levels of the wag are allowed as Type B bands ($A_2 \times B_2 = B_1$ which gives

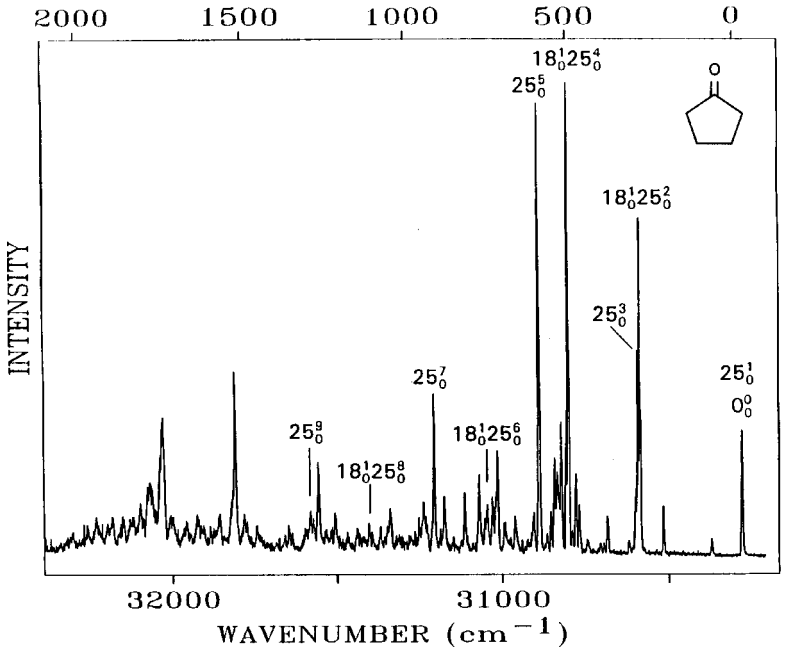

Figure 24. FES of CP [60].

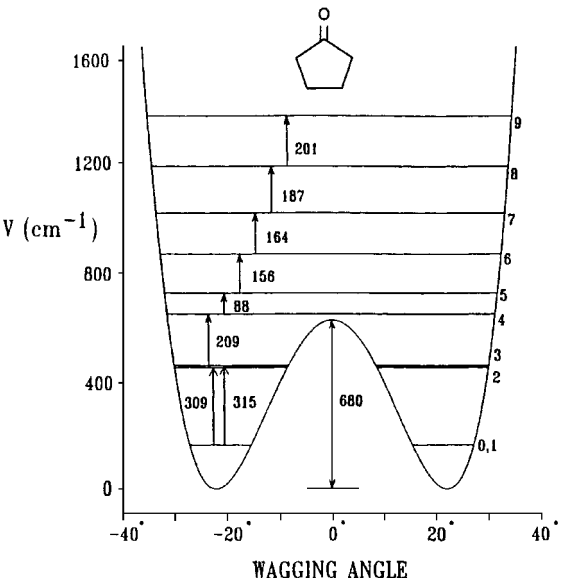

Figure 25. C=O wagging potential energy function for CP in its excited state [60].

the Type B band type). As it turns out, the barrier to inversion of the carbonyl group in CB is sufficiently high that the lowest six pairs of levels are nearly doubly degenerate with vibrational symmetry species A_1 and B_2. Even though transitions involving only the vibrational states of B_2 symmetry can be observed, these have essentially identical frequencies as those involving the A_1 states.

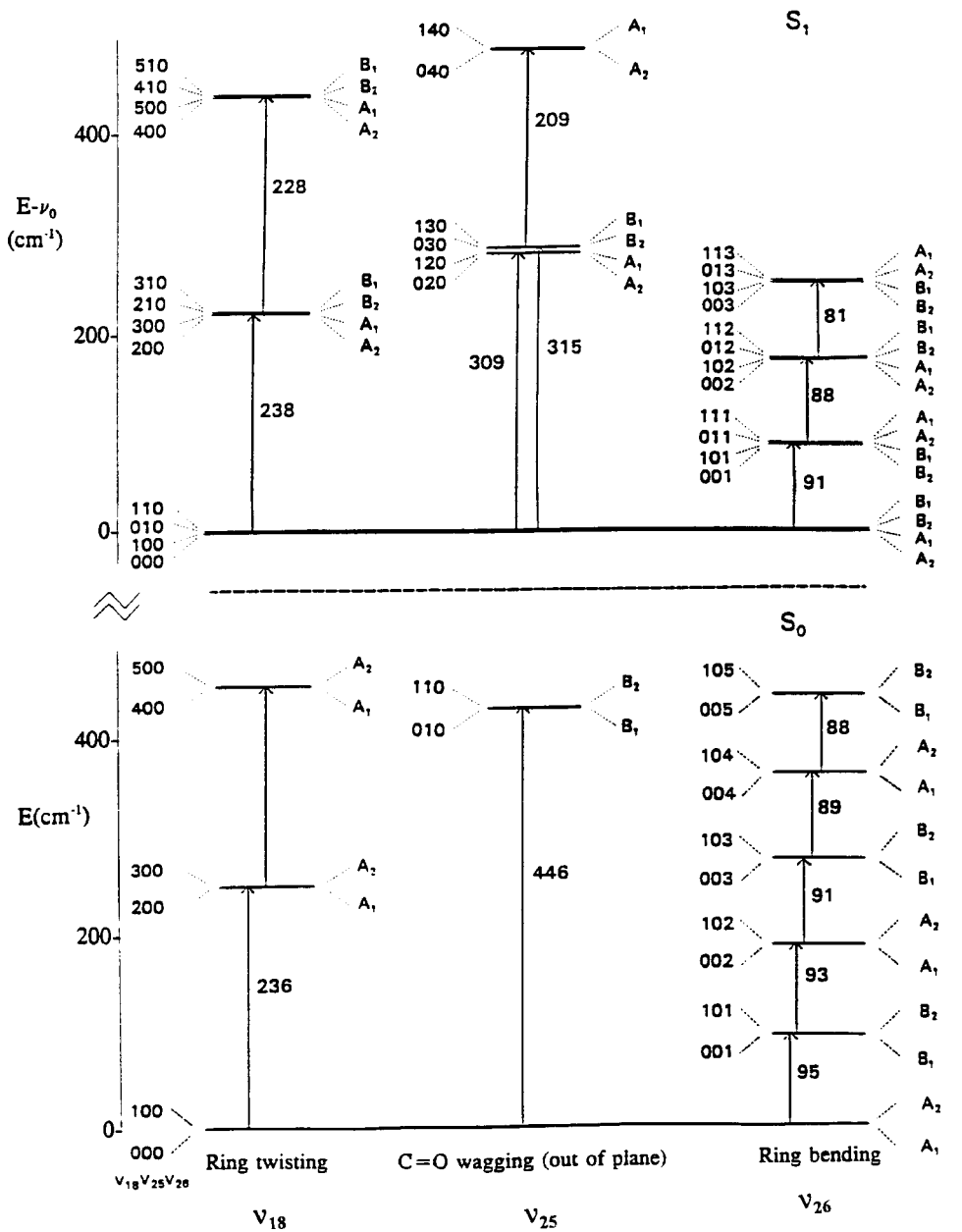

Figure 26. Energy level diagram for the ground and excited states of CP [61].

Figure 29 shows the C=O wagging potential energy function with a barrier of 2149 cm^{-1} and energy minima at $\pm 39°$. Table 3 presents the reduced mass and potential energy parameters for CB. The ring-puckering frequency shows a dramatic increase in going from 37 cm^{-1} in the S_0 state to 106 cm^{-1} in the excited state. This is in part due to the asymmetry associated with the puckering motion in the excited state resulting from its relationship to the carbonyl group. We have used data for the ring-puckering in the electronic excited state along with the carbonyl wagging

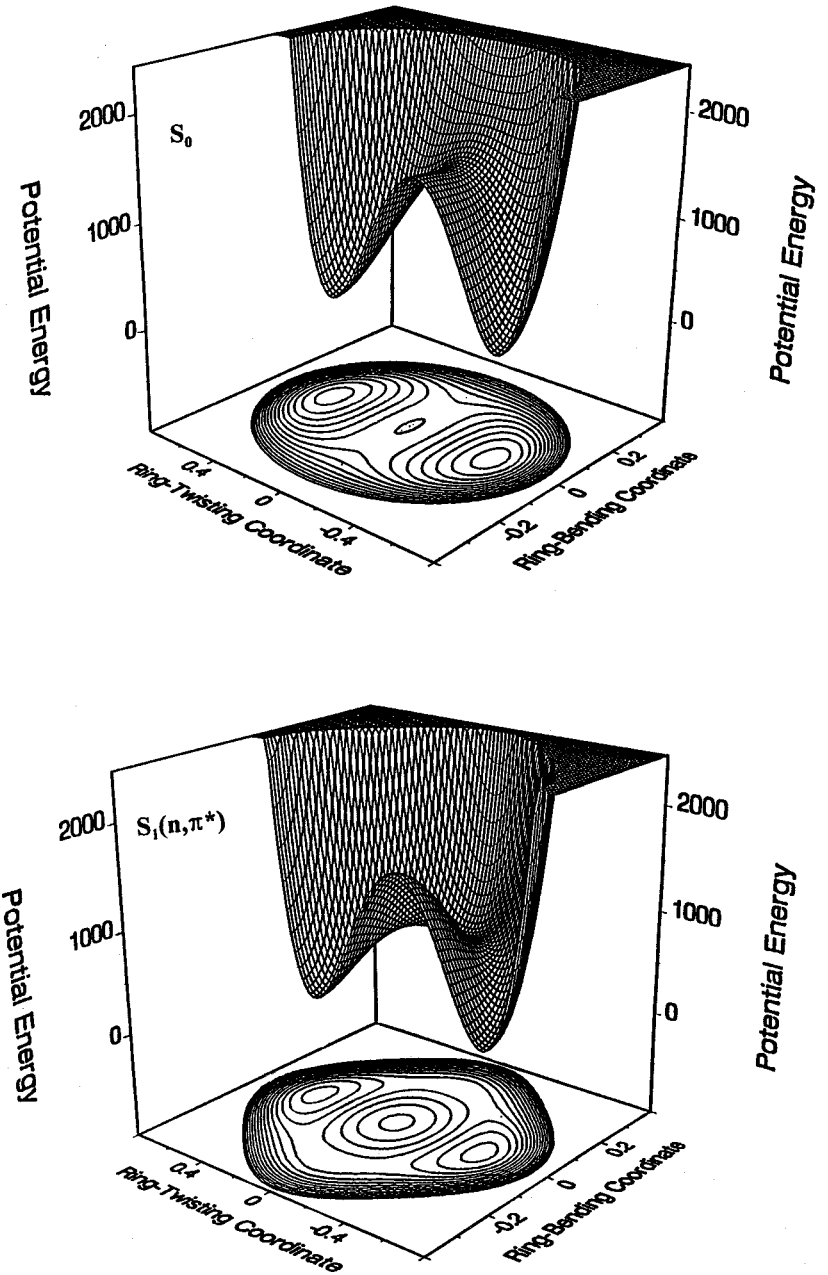

Figure 27. Vibrational potential energy surface for the ring-bending and ring-twisting of CP in its S_0 and S_1 states [61].

data to determine the two-dimensional puckering/ wagging potential energy surface, and this is shown elsewhere [62].

The data on the vibrational potential energy functions for several other cyclic ketones which we have studied are shown in table 3. Figure 30 correlates the inversion barrier values with the CCC angle at the carbonyl carbon atom [63] and

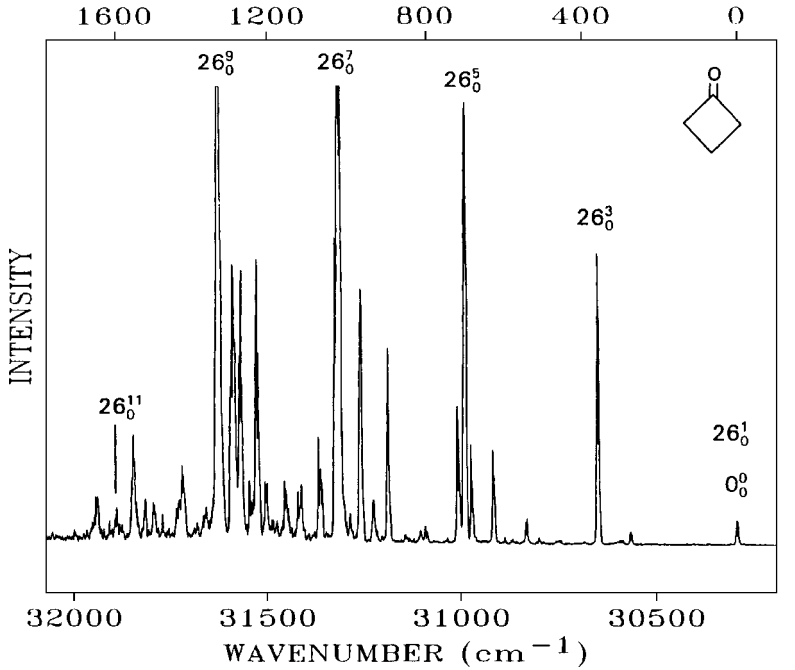

Figure 28. FES of CB [62].

also shows the equilibrium wagging angles. It is evident that increased angle strain, as measured by the difference between the actual ring angle and the 'desired' angle, results in increased barrier values. The frequency changes in the electronic excited state for several of the most sensitive vibrations are shown in table 2.

3.4. *Potential energy surfaces for phthalan and 1,3-benzodioxole*

We have recently initiated a comprehensive study of several bicyclic molecules of the indan family (scheme 3). These molecules are of interest in that they have highly interactive ring-puckering and ring-flapping modes, and they can be readily studied in both their ground and $S_1(\pi, \pi^*)$ excited states. These investigations have included the recording of far-infrared spectra, Raman spectra, mid-infrared combination band spectra, electronic absorption spectra, and both the fluorescence excitation spectra and dispersed fluorescence spectra of jet-cooled molecules. The results for phthalan and 1,3-benzodioxole (BZD) will be reported here.

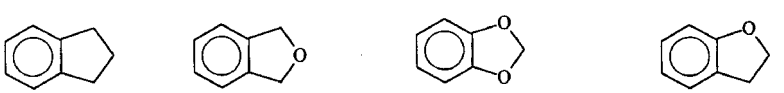

Scheme 3

Each of these molecules has three low-frequency out-of-plane ring vibrations. The vibrational coordinates for the ring-puckering and flapping are shown in figure 31. These have the same symmetry species (B_2) and interact strongly. The third vibration, the ring-twisting has A_2 symmetry and does not significantly couple to the other two modes. The puckering–flapping interaction was found to occur primarily through

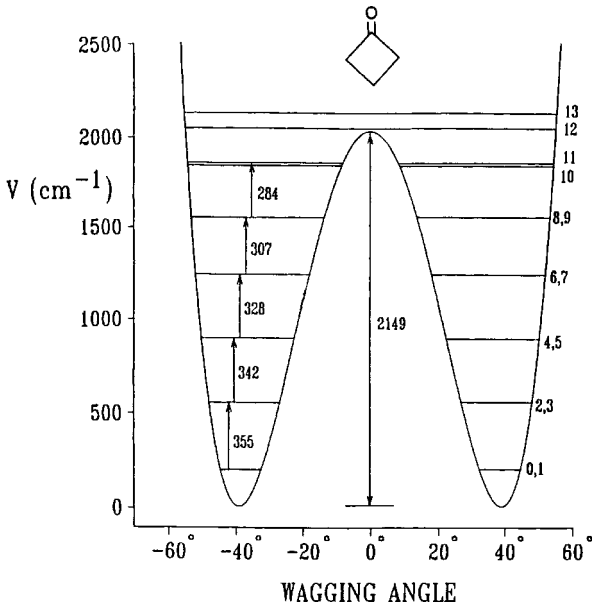

Figure 29. Carbonyl wagging potential energy function for CB [62].

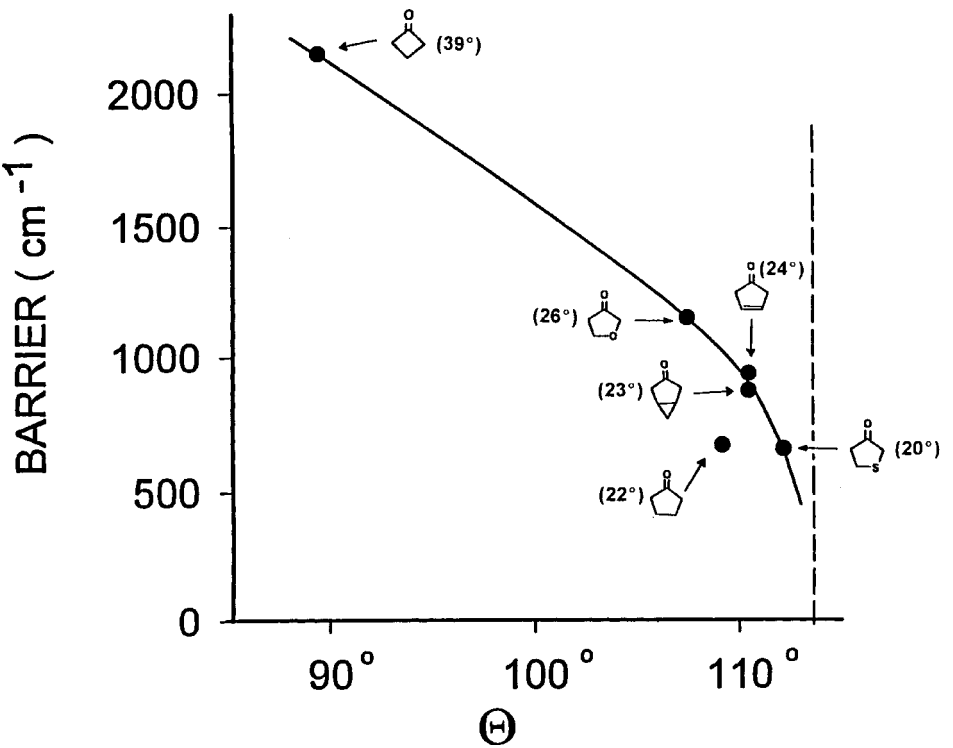

Figure 30. Correlation of inversion barrier with CCC angle at the carbonyl carbon atom. The dashed line indicates the 'strain free' angle. The equilibrium wagging angles for each molecule are shown in parentheses.

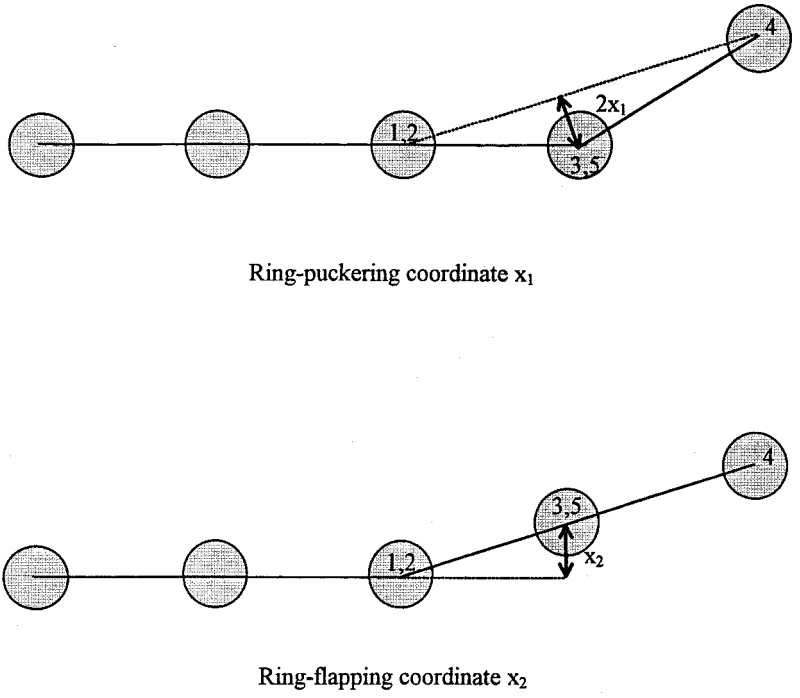

Figure 31. Definition of the ring-puckering (x_1) and ring-flapping (x_2) coordinates.

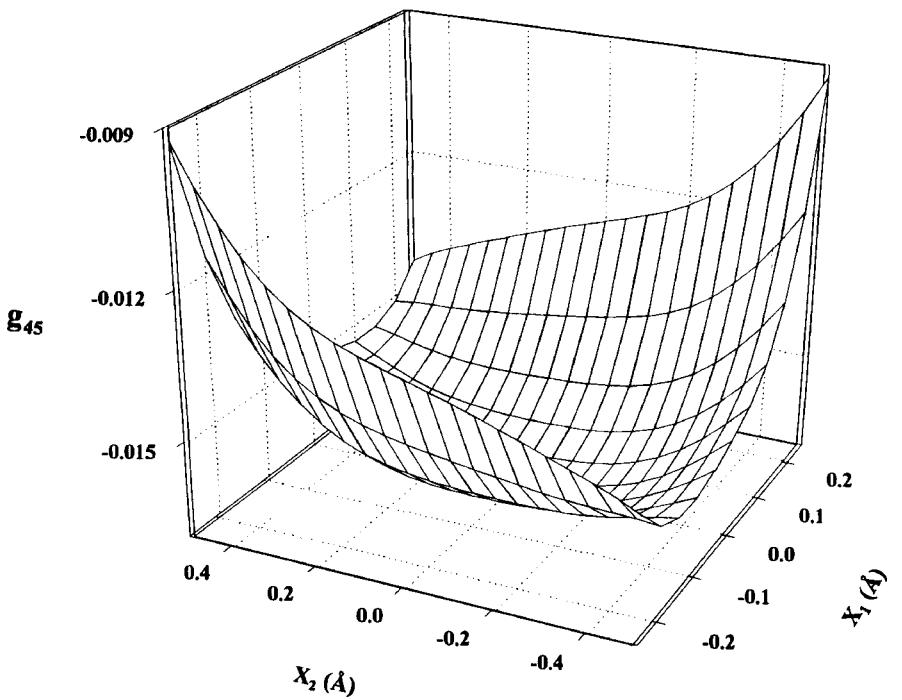

Figure 32. Dependence of the kinetic energy interaction term on the vibrational coordinates [66].

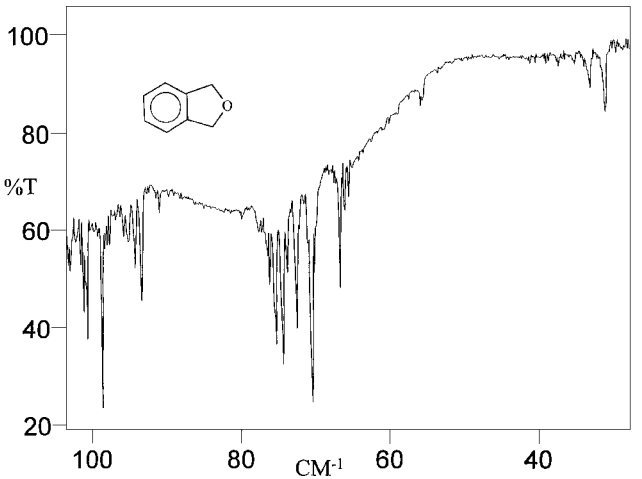

Figure 33. Far-infrared spectrum of phthalan [65].

the cross-kinetic energy term g_{45} [65, 66].All of the kinetic energy expressions (reciprocal reduced masses) were found to be highly coordinate dependent. As an example, figure 32 shows how g_{45} varies as a function of the puckering (x_1) and flapping (x_2) coordinates. This has the mathematical form

$$g_{45} = -0.01670 + 0.03006x_1^2 + 0.5854x_1^4 - 1.317x_1^6 + 0.002971x_2^2 + 0.02645x_2^4 - 0.04366x_2^6 - 0.04506x_1^2x_2^2 - 0.04241x_1^3x_2 + 0.1666x_1x_2^3 . \quad (19)$$

Figure 33 shows a portion of the far-infrared spectrum of phthalan from which the energy level diagram for the puckering and flapping levels shown in figure 34 was determined [65]. The puckering levels can be fit only moderately well using the one-dimensional potential energy function of the type given in equation (4). In particular, the irregular pattern caused by the 98.5 and 93.2 cm^{-1} transitions, whose assignments were confirmed by combination and overtone bands, cannot be reproduced. However, a two-dimensional calculation using the coordinate dependent kinetic energy functions such as that in equation (19) readily reproduces the irregular pattern. Figure 35 shows the two-dimensional potential energy surface which can be used to fit all the data very nicely. This has the form of equation (15). The potential energy surface has a barrier to planarity of 35 cm^{-1}, but the molecule is planar since the puckering zero-point energy is higher than the barrier.

Figure 36 shows the fluorescence excitation spectra of jet-cooled phthalan along with the electronic absorption spectra recorded at room temperature [67]. Dispersed fluorescence spectra from several excitation lines were recorded and these serve to confirm the ground state assignments. Analysis of the excitation spectra and the absorption spectra leads to the assignment of the puckering levels in the $S_1(\pi,\pi^*)$ excited states. Figure 37 presents the one-dimensional function which can be determined from these levels. The figure also compares the S_1 potential energy along the puckering coordinate to that in the electronic ground state. Rather surprisingly, the ring is somewhat stiffer in the excited state.

The investigation of 1,3-benzodioxole (BZD) was carried out in a similar manner [68]. This molecule is particularly interesting in that BZD, like 1,3-dioxole discussed earlier, has the anomeric effect present to influence its structure. Without this effect,

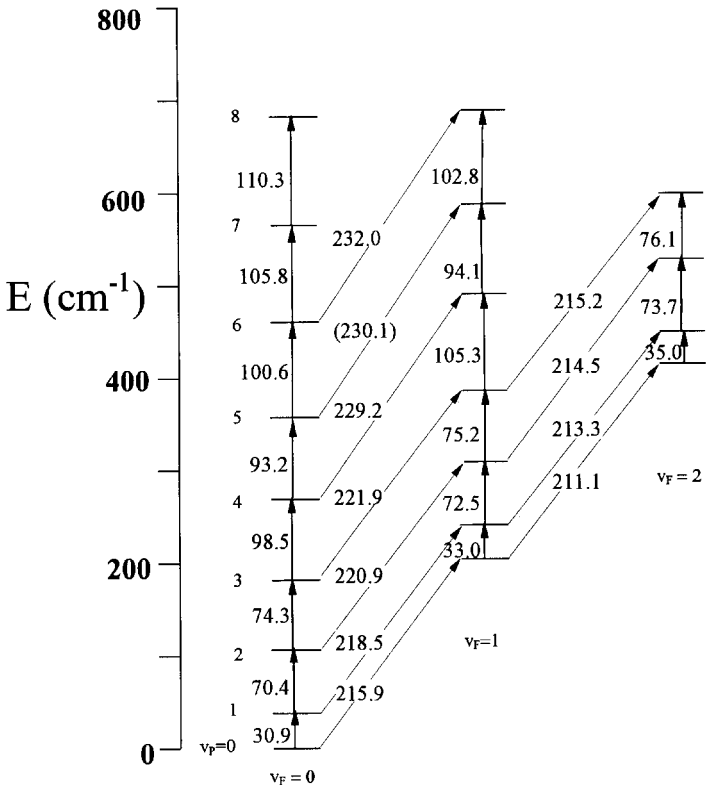

Figure 34. Energy level diagram for the ring-puckering and flapping of phthalan [65].

the molecule is expected to be planar. Figure 38 shows the far-infrared spectrum of BZD and figure 39 shows the Raman spectrum, which shows the double quantum jumps and the ring-twisting band at 214 cm^{-1}. As was the case for phthalan, BZD has strong coupling between the puckering and the flapping modes, but here the coupling is primarily through potential energy interactions. Figure 40 shows the puckering-flapping energy diagram determined from the spectra, and the puckering levels in the flapping excited state can be seen to be perturbed dramatically. Figure 41 shows the potential energy surface determined from this data. The barrier to inversion is 165 cm^{-1} and the dihedral angle of puckering is 26°. The ring also appears to have a flapping angle of 3°. The barrier here is only about one-half of that in 1,3-dioxole showing that the presence of the benzene ring reduces the magnitude of the anomeric effect. The electronic excited state of BZD is currently under investigation as are the ground and excited states of indan and coumeran.

3.5. *trans-Stilbene*

For more than two decades the photoisomerization of stilbene has been of great interest to both theoretical and experimental chemists (see [69] and references therein). It is generally believed that the isomerization is facilitated in the electronic excited state by the internal rotation about the C=C bond, which has a potential energy minimum corresponding to a perpendicular (twisted) configuration (analogous to the ethylene D_{2d} structure in its $S_1(\pi, \pi^*)$ state). A barrier of about 1200 cm^{-1}

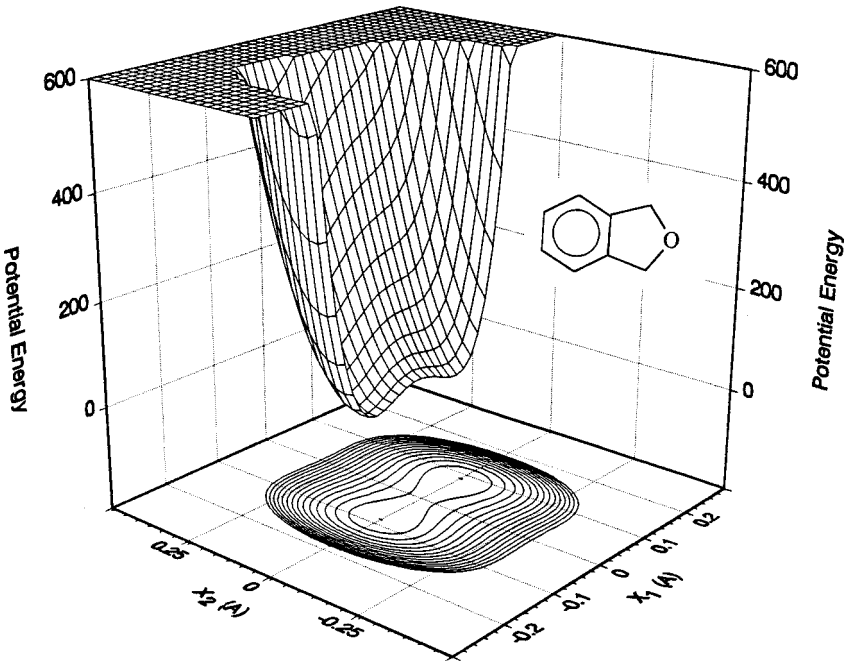

Figure 35. Two-dimensional potential energy surface for phthalan in terms of the ring-puckering (x_1) and ring-flapping (x_2) coordinates [66].

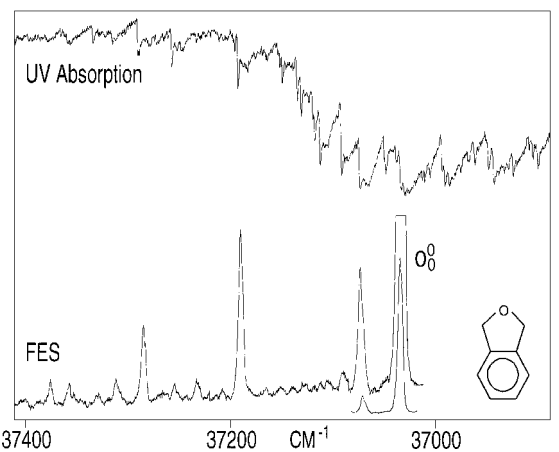

Figure 36. Electronic absorption spectra (25°C) and fluorescence excitation spectra of jet-cooled phthalan.

hindering the *trans* to twist internal rotation was determined for the S_1 state by Bánares *et al.* [70]. Because the dynamics of the photoisomerization is strongly affected by the vibrational potential energy surfaces, there has been considerable interest in assigning the vibrational spectra of *trans*-stilbene, especially for the torsional modes, for both the ground (S_0) and excited (S_1) electronic states. However, there had not been general agreement on the vibrational frequencies associated with

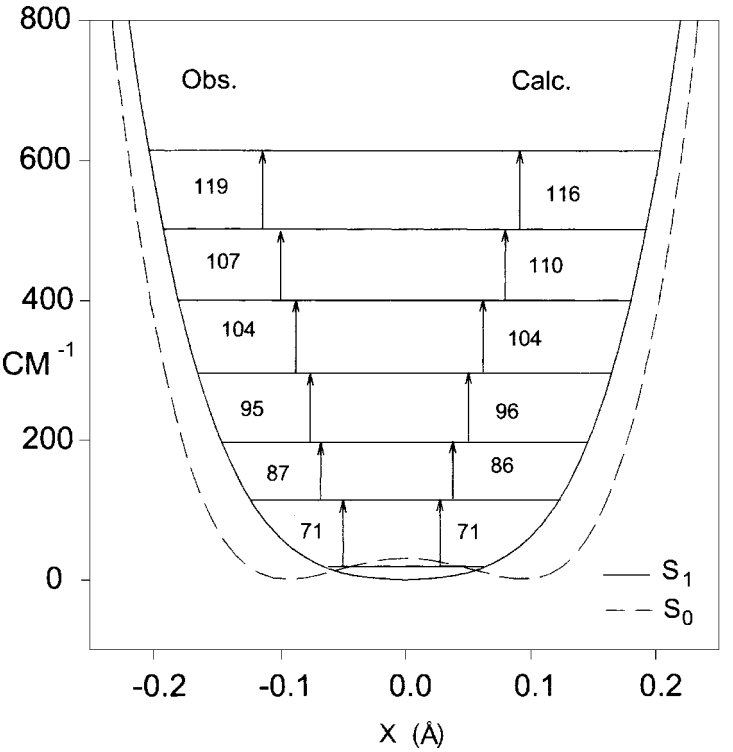

Figure 37. Ring-puckering potential energy function for the $S_1(\pi,\pi^*)$ excited state of phthalan compared to the ground state potential energy function.

each mode. Several groups proposed frequency assignments and Waldeck [71] has reviewed this work.

We have recently reinvestigated [69] the fluorescence excitation (figure 42) and dispersed fluorescence spectra (figure 43) and used these, together with high-temperature vapour-phase Raman data [72] to reassign the eight low-frequency (below 300 cm^{-1}) vibrations of this molecule in its S_0 and $S_1(\pi,\pi^*)$ states. These vibrations are shown in figure 44. We then carried out kinetic energy (reciprocal reduced mass) calculations for the two phenyl torsions ν_{37} and ν_{48}, and utilized these results along with the experimental data to determine the two-dimensional potential energy surfaces for these modes in both the S_0 and S_1 states. The function

$$V(\phi_1, \phi_2) = \tfrac{1}{2}V_2(2 + \cos 2\phi_1 + \cos 2\phi_2) + V_{12}\cos 2\phi_1 \cos 2\phi_2 + V'_{12}\sin 2\phi_1 \sin 2\phi_2 , \quad (20)$$

with $V_2 = 1550\,cm^{-1}$, $V_{12} = 337.5\,cm^{-1}$ and $V'_{12} = 402.5\,cm^{-1}$ for the S_0 state and with $V_2 = 1500\,cm^{-1}$, $V_{12} = 85\,cm^{-1}$, and $V'_{12} = 55\,cm^{-1}$ for the $S_1(\pi, \pi^*)$ state fits the observed data (nine frequencies for S_0, six for S_1) extremely well. The barriers to simultaneous internal rotation of both phenyl groups are given by twice the V_2 values. The fundamental frequencies for these torsions are $\nu_{37} = 9\,cm^{-1}$ and $\nu_{48} = 118\,cm^{-1}$ for the S_0 state and $\nu_{37} = 35\,cm^{-1}$ and $\nu_{48} = 110\,cm^{-1}$ for the S_1 excited state. Figure 45 presents the potential energy surface for the phenyl torsions in the S_1 state. This surface has four equivalent energy minima and results in a four-fold degeneracy of each of the phenyl torsional states.

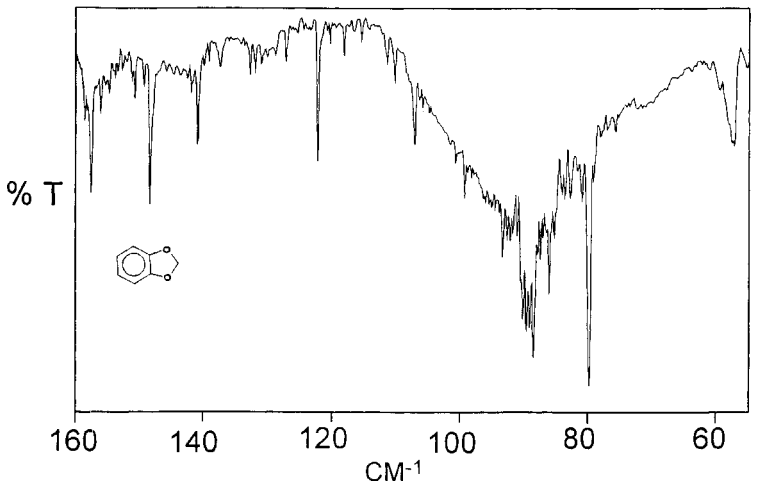

Figure 38. Far infrared spectrum of BZD [68].

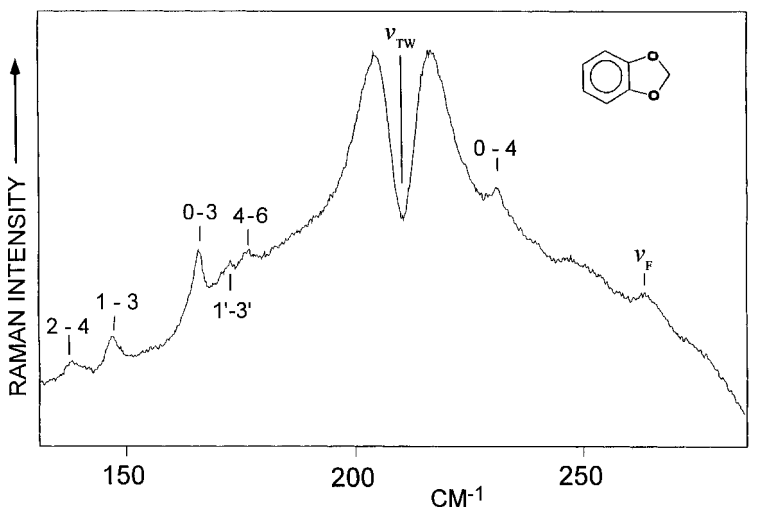

Figure 39. Raman spectrum of BZD at 200°C [68].

The third torsion, ν_{35}, which is the internal rotation about the C=C bond, was assigned at 101 cm^{-1} for the S_0 state based on a series of overtone frequencies (202 cm^{-1}, 404 cm^{-1}, etc.). For S_1 ν_{35} = 99 cm^{-1} based on observed frequencies at 198, 396 cm^{-1}, etc. Kinetic energy calculations were also carried out for this mode, and a one-dimensional potential energy function of the form

$$V(\theta) = \tfrac{1}{2}V_1(1 - \cos\theta) + \tfrac{1}{2}V_2(1 - \cos 2\theta) + \tfrac{1}{2}V_4(1 - \cos 4\theta) \qquad (21)$$

was utilized to reproduce the frequencies for the ground state. Since the observed vibrational levels extend to less than 3 kcal mol^{-1} beyond the potential energy minimum in the S_0 state, they can only be used to approximate the torsional barrier which was calculated to be 50 ± 20 kcal mol^{-1}. This is in general agreement with the accepted value of 48 kcal mol^{-1} [71, 73]. For the S_1 excited state an additional

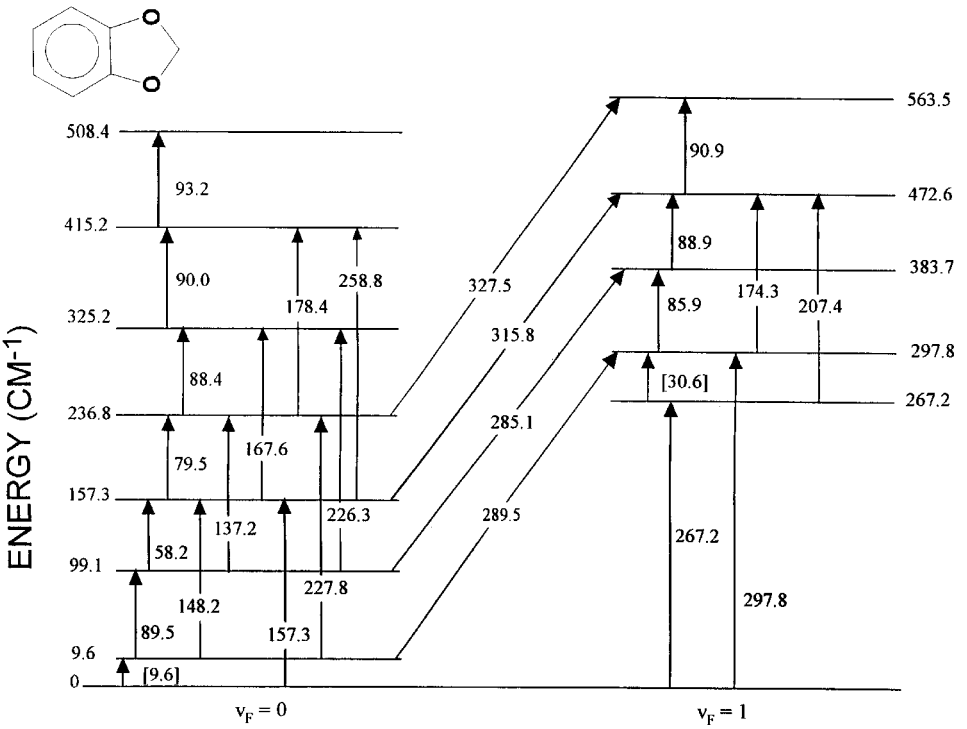

Figure 40. Ring-puckering and flapping levels of BZD [68].

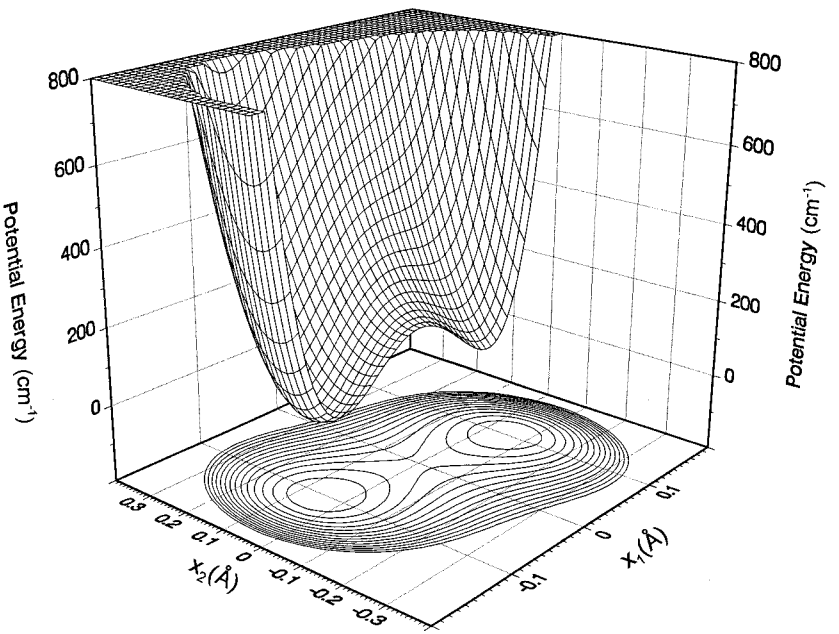

Figure 41. Vibrational potential energy surface for the ring-puckering and flapping of BZD [68].

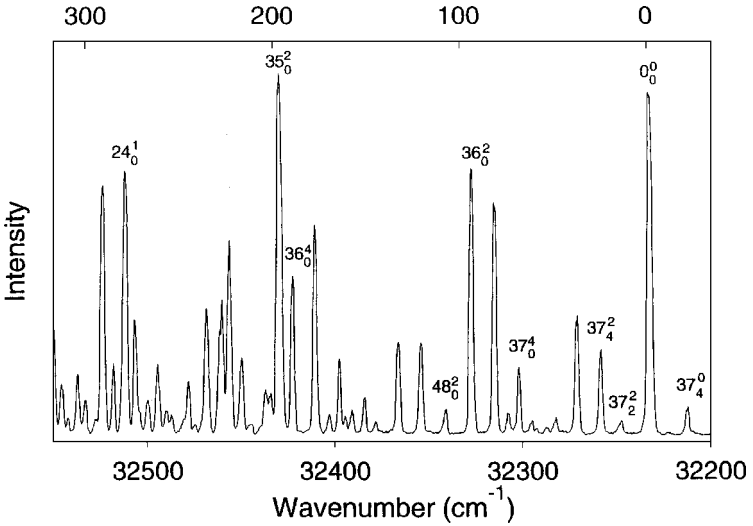

Figure 42. Fluorescence excitation spectrum of *trans*-stilbene [69].

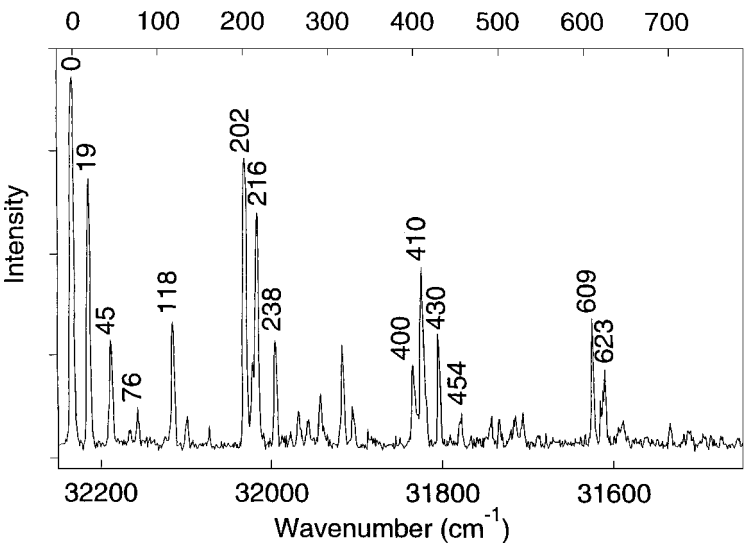

Figure 43. Dispersed fluorescence spectrum of *trans*-stilbene recorded from the electronic band origin [69].

V_8 term was added to equation (21) in order to fit the data for the *trans* potential energy well. The data indicate that the *trans* $\rightarrow$ twist barrier for the S_1 state is between 1400 and 2000 cm^{-1}. This is compatible with the dynamics study [70] where the isomerization rate begins to increase dramatically when the excess energy reaches 1200 cm^{-1}. Near the top of the barrier tunnelling is expected to increase the photoisomerization rate, which becomes even more substantial above the barrier. Figure 46 shows the potential energy for the ethylinic torsion for both the ground

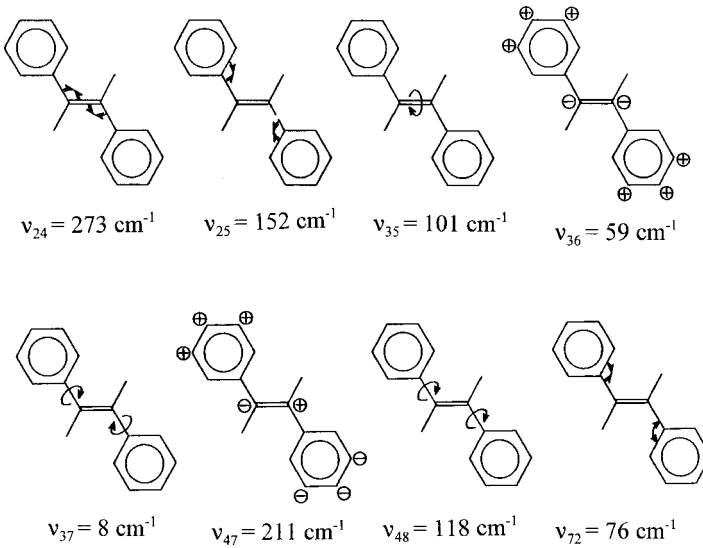

Figure 44. Low-frequency vibrations of *trans*-stilbene.

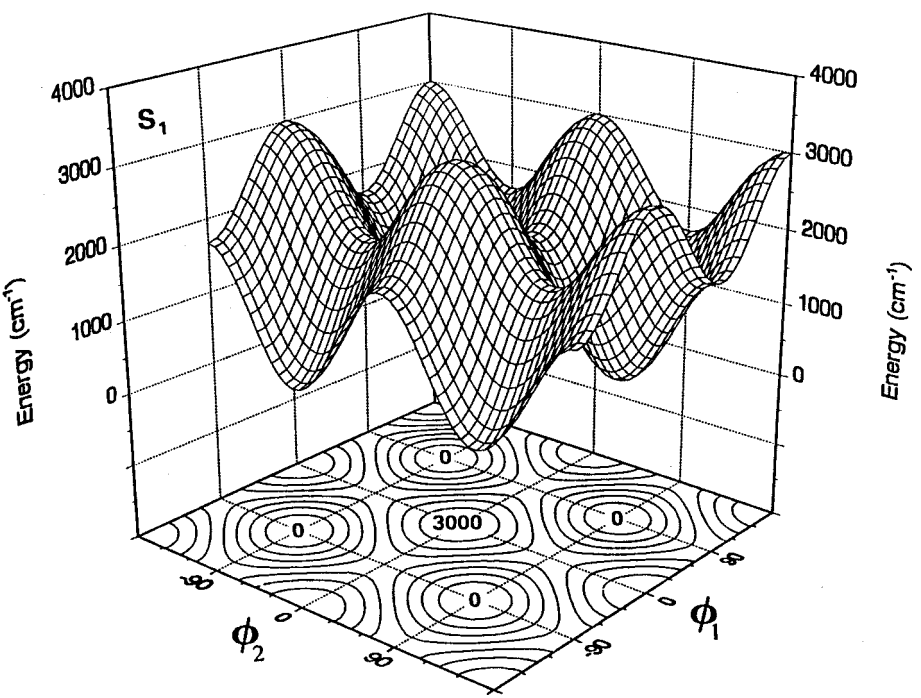

Figure 45. Potential energy surface for the phenyl torsions of *trans*-stilbene in its S_1 state [69].

and excited state [69]. It can be seen how the relatively low *trans* $\rightarrow$ twist barrier facilitates the photoisomerization in the electronic excited state.

Work on other stilbenes is in progress. The results for methoxy-*trans*-stilbene have been published, and these support the conclusions drawn for the *trans*-stilbene [74].

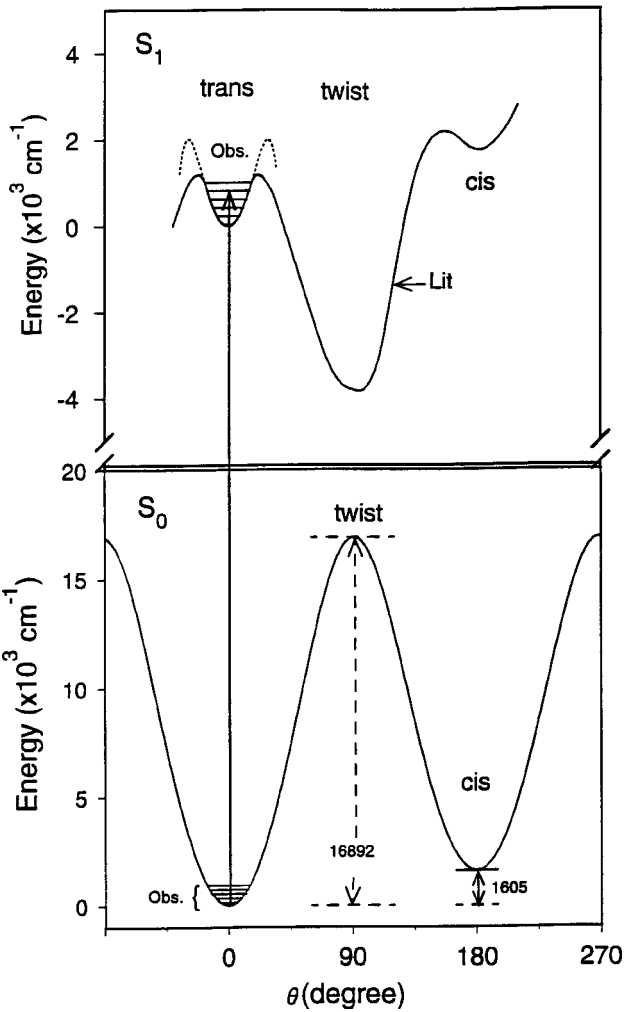

Figure 46. Potential energy function for the internal rotation about the C=C bond for the ground and excited states of *trans*-stilbene [69].

4. Conclusion

Selected vibrations in several types of molecules can be studied by spectroscopic methods in order to understand the conformational energetics and interconversions of these molecules. In the electronic ground state, far-infrared and Raman spectra, complemented by dispersed fluorescence and/or electronic absorption spectra can be utilized to determine the conformationally important quantum states. In some cases, such as the ring-puckering of four-membered and psuedo-four-membered rings, a one-dimensional potential energy function can be utilized to fit the spectral data. Such potential functions establish the conformation of the molecule and provide the barriers to conformational changes (if any). The potential energy parameters can also be used to better understand the intramolecular forces and often allow unusual effects, such as the anomeric effect, to be quantitatively evaluated. For saturated five-membered rings, cyclohexene-type molecules, and various other types of

molecules where two conformationally important vibrational pathways are present, more complicated two-dimensional potential energy surfaces are required for the analyses.

For electronic excited states, similar analyses can be carried out surprisingly well. Fluorescence excitation spectra of jet-cooled molecules together with electronic absorption spectra can be used to determine the conformationally important vibrational quantum states in electronic excited states. Our work has focused on ketones with their $S_1(n,\pi^*)$ excited states and on various aromatic systems with their $S_1(\pi,\pi^*)$ states. Analysis of the potential energy functions for carbonyl wagging modes or of the potential energy surfaces of ring modes or torsions provides considerable insight into the structures and dynamical processes that occur in these excited states.

Acknowledgments

Financial support from the National Science Foundation, the Robert A. Welch Foundation, and the Texas ARP program is gratefully acknowledged. The work described here was carried out by the able graduate students and research associates who are referenced herein. Dr Soo-No Lee helped with the preparation of the figures.

References

[1] Morse, P. M., 1929, *Phys. Rev.*, **34,** 57.
[2] Wilson, E. B., Decius, and Cross, P. C., 1955, *Molecular Vibrations*, 289.
[3] Burkett, U., and Allinger, N. L., 1982, *Molecular Mechanics*, American Chemical Society Monograph (Washington, DC: ACS).
[4] Dennison, D. M., 1940, *Rev. mod. Phys.*, **12,** 175.
[5] Manning, M. F., 1935, *J. chem. Phys.*, **3,** 136.
[6] Laane, J., 1970, *Appl. Spectrosc.*, **24,** 73.
[7] Coon, J. B., Naugle, N. W., and McKenzie, R. D., 1966, *J. molec. Spectrosc.*, **20,** 107.
[8] Laane, J., 1971, *Quart. Rev.*, **25,** 533.
[9] Laane, J., 1972, *Vibrational Spectra and Structure*, edited by J. R. Durig (New York: Marcel Dekker), p. 25.
[10] Laane, J., 1987, *Pure appl. Chem.*, **59,** 1307.
[11] Laane, J., 1993, *Structures and Conformations of Non-Rigid Molecules*, edited by J. Laane, M. Dakkouri, B. van der Veken and H. Oberhammer (Amersterdam: Kluwer Publishing), p. 65.
[12] Laane, J., 1994, *Ann. Rev. Phys. Chem.*, **45,** 179.
[13] Harthcock, M. A., and Laane, J., 1982, *J. molec. Spectrosc.*, **94,** 461.
[14] Villarreal, J. R., Bauman, L. E., and Laane, J., 1976, *J. chem. Phys.*, **80,** 1172.
[15] Bauman, L. E., Killough, P. M., Cooke, J. M., Villarreal, J. R., and Laane, J., 1982, *J. phys. Chem.*, **82,** 2000.
[16] Killough, P. M., Irwin, R. M., and Laane, J., 1982, *J. chem. Phys.*, **76,** 3890.
[17] Jagodzinski, P. W., Richardson, L. W., Harthcock, M. A., and Laane, J., 1980, *J. chem. Phys.*, **73,** 5556.
[18] Harthcock, M. A., and Laane, J., 1983, *J. chem. Phys.*, **79,** 2103.
[19] Strube, M. M., and Laane, J., 1988, *J. molec. Spectrosc.*, **129,** 126.
[20] Laane, J., Harthcock, M. A., Killough, P. M., Bauman, L. E., and Cooke, J. M., 1982, *J. molec. Spectrosc.*, **91,** 286.
[21] Harthcock, M. A., and Laane, J., 1982, *J. molec. Spectrosc.*, **91,** 300.
[22] Schmude, R. W., Harthcock, M. A., Kelly, M. B., and Laane, J., 1987, *J. molec. Spectrosc.*, **124,** 369.
[23] Tecklenburg, M. M., and Laane, J., 1989, *J. molec. Spectrosc.*, **137,** 65.
[24] Bell, R. P., 1945, *Proc. Roy. Soc.*, **A183,** 328.
[25] Laane, J., 1991, *J. phys. Chem.*, **95,** 9246.
[26] Harhcock, M., and Laane, J., 1982, *J. phys. Chem.*, **86,** 2000.
[27] Danti, A., Lafferty, W. J., and Lord, R. C., 1960, *J. chem. Phys.*, **33,** 294.

[28] CHAN, S., ZINN, J., FERNANDEZ, J., and GWINN, W. D., 1960, *J. chem. Phys.*, **33,** 1643; CHAN, S., ZINN, J., and GWINN, W. D., 1961, *J. chem. Phys.*, **34,** 1319.
[29] CHAN, S. I., BORGERS, T. R., RUSSELL, J. W., STRAUSS, H. L., and GWINN, W. D., 1961, *J. Chem. Phys. Chem.*, **44,** 1103.
[30] BORGERS, T. R., and STRAUSS, H. L., 1966, *J. chem. Phys.*, **45,** 947.
[31] LAANE, J., and LORD, R. C., 1968, *J. chem. Phys.*, **48,** 1508.
[32] LAANE, J., and LORD, R. C., 1967, *J. chem. Phys.*, **47,** 4941.
[33] LAANE, J., and LORD, R. C., 1971, *J. molec. Spectrosc.*, **39,** 340.
[34] CORTEZ, E., VERASTEGUI, R., VILLARREAL, J. R., and LAANE, J., 1993, *J. Am. chem. Soc.*, **115,** 12132.
[35] LAANE, J., 1969, *J. chem. Phys.*, **50,** 776.
[36] KILLOUGH, P. M., and LAANE, J., 1984, *J. chem. Phys.*, **80,** 5475.
[37] BAUMAN, L. E., KILLOUGH, P. M., COOKE, J. M., VILLARREAL, J. R., and LAANE, J., 1982, *J. phys. Chem.*, **86,** 2000.
[38] LAANE, J., 1970, *J. chem. Phys.*, **52,** 358.
[39] KELLY, M. B., and LAANE, J., 1988, *J. chem. Phys.*, **92,** 4056.
[40] COLEGROVE, L. C., and LAANE, J., 1991, *J. phys. Chem.*, **95,** 6494.
[41] DEL ROSARIO, A., BITSCHENAUER, R., DAKKOURI, M., HALLER, K., and LAANE, J., 1998, *J. phys. Chem.*, **102,** 10261.
[42] KILPATRICK, J. E., PITZER, K. S., and SPITZER, R., 1947, *J. Am. chem. Soc.*, **75,** 5634; PITZER, K. S., and DONATH, W., 1959, *J. Am. chem. Soc.*, **81,** 3213.
[43] DURIG, J. R., and WERTZ, D. W., 1968, *J. chem. Phys.*, **49,** 2118.
[44] BAUMAN, L. E., and LAANE, J., 1988, *J. phys. Chem.*, **92,** 1040.
[45] COLEGROVE, L. F., WELLS, J. C., and LAANE, J., 1990, *J. chem. Phys.*, **93,** 6291.
[46] LEIBOWITZ, S. J., VILLARREAL, J. R., and LAANE, J., 1992, *J. chem. Phys.*, **96,** 7298.
[47] LEIBOWITZ, S. J., VILLARREAL, J. R., and LAANE, J., 1992, *J. phys. Chem.*, **96,** 8817.
[48] LEIBOWITZ, S. J., and LAANE, J., 1994, *J. chem. Phys.*, **101,** 2740.
[49] GAINES, V. E., LEIBOWITZ, S. J., and LAANE, J., 1991, *J. Am. chem. Soc.*, **113,** 9735.
[50] TECKLENBURG, M. M., and LAANE, J., 1993, *J. Am. chem. Soc.*, **111,** 6920.
[51] TECKLENBURG, M. M., VILLARREAL, J., and LAANE, J., 1989, *J. chem. Phys.*, **91,** 2771.
[52] CHEATHAM, C. M., HUANG, M.-H., MEINANDER, N., KELLY, M. B., HALLER, K., CHIANG, W.-Y., and LAANE, J., 1996, *J. molec. Struct.*, **377,** 81.
[53] CHEATHAM, C. M., HUANG, M.-H., and LAANE, J., 1996, *J. molec. Struct.*, **377,** 93.
[54] MORRIS, K., and LAANE, J., 1999, to be published.
[55] WALSH, A. D., 1953, *J. chem. Soc.*, 2306.
[56] BRAND, J. C. D., 1956, *J. chem. Soc.*, 858.
[57] CHEATHAM, C. M., and LAANE, J., 1991, *J. chem. Phys.*, **94,** 5394.
[58] CHEATHAM, C. M., and LAANE, J., 1991, *J. chem. Phys.*, **94,** 7743.
[59] SAGEAR, P., and LAANE, J., 1995, *J. chem. Phys.*, **102,** 7789.
[60] ZHANG, J., CHIANG, W.-Y., and LAANE, J., 1993, *J. chem. Phys.*, **98,** 6129.
[61] CHOO, J., and LAANE, J., 1994, *J. chem. Phys.*, **101,** 2772.
[62] ZHANG, J., CHIANG, W.-Y., and LAANE, J., 1994, *J. chem. Phys.*, **100,** 3455.
[63] SAGEAR, P., LEE, S. N., and LAANE, J., 1997, *J. chem. Phys.*, **106,** 3876.
[64] CHIANG, W.-Y., and LAANE, J., 1995, *J. phys. Chem.*, **99,** 11640.
[65] KLOTS, T., SAKURAI, S., and LAANE, J., 1998, *J. chem. Phys.*, **108,** 3531.
[66] SAKURAI, S., MEINANDER, N., and LAANE, J., 1998, *J. chem. Phys.*, **108,** 3537.
[67] SAKURAI, S., BONDOC, E., MORRIS, K., CHIANG, W.-Y., and LAANE, J., 1999, *J. chem. Phys.*, to be published.
[68] SAKURAI, S., and LAANE, J., 1999, *J. Am. chem. Soc.*, to be published.
[69] CHIANG, W.-Y., and LAANE, J., 1994, *J. chem. Phys.*, **101,** 8755.
[70] BÅNARES, L, HEIKAL, A. A., and ZEWAIL, A. H., 1992, *J. chem. Phys.*, **96,** 4127.
[71] WALDECK, D. H., 1991, *Chem. Rev.*, **91,** 415.
[72] HALLER, K, CHIANG, W.-Y., DEL ROSARIO, A., and LAANE, J., 1996, *J. molec. Struct.*, **379,** 19.
[73] SALTIEL, J., GANAPATHY, S., and WERKING, C., 1987, *J. phys. Chem.*, **90,** 2755.
[74] CHIANG, W.-Y., and LAANE, J., 1995, *J. phys. Chem.*, **99,** 11823.